

1 ACCURATE AND SENSITIVE DETERMINATION OF MOLAR FRACTIONS OF <sup>13</sup>C-  
2 LABELLED INTRACELLULAR METABOLITES IN CELL CULTURES GROWN IN  
3 THE PRESENCE OF ISOTOPICALLY-LABELLED GLUCOSE

4 Mario Fernández-Fernández<sup>a</sup>, Pablo Rodríguez-González\*<sup>a</sup>, David Hevia Sánchez<sup>b</sup>, Pedro  
5 González-Menéndez<sup>b</sup>, Rosa M<sup>a</sup> Sainz Menéndez<sup>b</sup>, J. Ignacio García Alonso<sup>a</sup>.

6 <sup>a</sup>*Department of Physical and Analytical Chemistry. Faculty of Chemistry. University of Oviedo.*  
7 *Julián Clavería 8, 33006 Oviedo, Spain.*

8 <sup>b</sup>*University Institute of Oncology (IUOPA), University of Oviedo. Julián Clavería 6, 33006 Oviedo,*  
9 *Spain.*

10 \*Author for correspondence: [rodriguezpablo@uniovi.es](mailto:rodriguezpablo@uniovi.es)

11 Postal address: Department of Physical and Analytical Chemistry. Faculty of Chemistry. University of  
12 Oviedo. Julián Clavería 8, 33006 Oviedo, Spain.

13 Phone number: +34 985103000-5366

14 Fax number: +34 985103125

15

16 **ABSTRACT**

17 This work describes a methodology based on multiple linear regression and GC-MS for the  
18 determination of molar fractions of isotopically-labeled intracellular metabolites in cell  
19 cultures. Novel aspects of this work are: i) the calculation of theoretical isotopic distributions  
20 of the different isotopologues from an experimentally measured value of %  $^{13}\text{C}$  enrichment  
21 of the labelled precursor ii) the calculation of the contribution of lack of mass resolution of  
22 the mass spectrometer and different fragmentation mechanism such as the loss or gain of  
23 hydrogen atoms in the EI source to measure the purity of the selected cluster for each  
24 metabolite and iii) the validation of the methodology not only by the analysis of  
25 gravimetrically prepared mixtures of isotopologues but also by the comparison of the  
26 obtained molar fractions with experimental values obtained by GC-Combustion-IRMS based  
27 on  $^{13}\text{C}/^{12}\text{C}$  isotope ratio measurements. The method is able to measure molar fractions for  
28 twenty-eight intracellular metabolites derived from glucose metabolism in cell cultures grown  
29 in the presence of  $^{13}\text{C}$ -labelled Glucose. The validation strategies demonstrate a satisfactory  
30 accuracy and precision of the proposed procedure. Also, our results show that the minimum  
31 value of  $^{13}\text{C}$  incorporation that can be accurately quantified is significantly influenced by the  
32 calculation of the spectral purity of the measured cluster and the number of  $^{13}\text{C}$  atoms of the  
33 labelled precursor. The proposed procedure was able to accurately quantify gravimetrically  
34 prepared mixtures of natural and labelled glucose molar fractions of 0.07% and mixtures of  
35 natural and labeled glycine at molar fractions down to 0.7%. The method was applied to  
36 initial studies of glucose metabolism of different prostate cancer cell lines.

37

38 **Keywords:** Glucose metabolism;  $^{13}\text{C}$ -labelled compounds; Multiple linear regression; Cell  
39 cultures; Prostate cancer.

40

## 41 1. INTRODUCTION

42 The relationship between cancer and glucose metabolism was first proposed by Otto  
43 Warburg<sup>1</sup> in 1920s when he discovered that carcinogenic cells consumed glucose faster than  
44 healthy cells via glycolysis. During the last decade, it was demonstrated that the increased  
45 glucose consumption of carcinogenic cells occurs not only via glycolysis but also via the  
46 pentose phosphate pathway<sup>2-4</sup>. Many of the current metabolomics approaches to study cell  
47 glucose metabolism make use of enriched stable-isotopes<sup>5-6</sup>. After the discovery of <sup>2</sup>H and  
48 <sup>15</sup>N by Urey<sup>9-10</sup>, the first studies of metabolic pathways using stable isotopes were carried out  
49 by Schoenheimer<sup>7-8</sup> in the 1930`s using <sup>2</sup>H- and <sup>15</sup>N-labeled compounds. After 1950, most of  
50 the metabolic pathway investigations were carried out using radiotracers due to the higher  
51 cost of stable isotopes<sup>11-12</sup>. However, during 1970`s radioactive isotopes were progressively  
52 replaced by stable isotopes<sup>13-14</sup> not only due to the associated health and environmental risks  
53 of working with radiotracers but also to the development of mass spectrometric techniques  
54 like GC-MS and LC-MS<sup>15</sup>. From the early 21<sup>st</sup>-century there has been a massive application  
55 of stable isotopes in metabolomics, and in particular in metabolic pathways investigations<sup>6</sup>.

56

57 Isotopic-fingerprinting of metabolites employs <sup>13</sup>C-labeled substrates to create specific  
58 labeling patterns in key metabolites to reveal metabolic pathways<sup>16</sup>. This usually includes  
59 three key steps. First, a <sup>13</sup>C-labeled tracer, in most cases <sup>13</sup>C-labeled glucose, is introduced  
60 into a growing cell culture. Then, <sup>13</sup>C-labeling is measured in intracellular metabolites and  
61 finally, individual biochemical pathways are estimated from the labeling patterns measured.  
62 This labeling strategy is mainly applied for several purposes: i) to confirm or discover  
63 functional pathways<sup>16</sup>, ii) to determine the contribution of a pathway in a synthesis product in  
64 metabolic engineering<sup>17</sup> and iii) to establish differences in metabolic routes between healthy  
65 and carcinogenic cells. Concerning the last application, <sup>13</sup>C-labeling can identify metabolic

66 changes due to a different proliferative status, to the presence of local or distant metastasis  
67 and after specific targeted therapies in cancer tissues<sup>18</sup>.

68

69 So far, two techniques are employed to measure the isotopic labeling in metabolites: Nuclear  
70 Magnetic Resonance (NMR) and Mass Spectrometry (MS) coupled to a chromatography  
71 separation such as LC-MS<sup>19</sup> or GC-MS<sup>20-24</sup> in combination with Mass Isotopomer  
72 Distribution Analysis (MIDA). NMR methods are less sensitive, require larger amount of  
73 sample and is mainly used to measured <sup>13</sup>C-positional enrichment<sup>25-26</sup>. MS is less expensive,  
74 and provides a more sensitive detection of the <sup>13</sup>C molecular enrichment<sup>27-29</sup>.

75

76 For the calculation of mass isotopologue distributions (MID), there are different approaches  
77 described in the literature. The first calculates MID directly from the integration of peak areas  
78 at each ion chromatogram to calculate fractional abundances<sup>20</sup>. In most cases<sup>30-35</sup> the peak  
79 areas are corrected for the natural abundance contribution of all elements contained in the  
80 molecule. The classical correction<sup>36</sup> assumes that MID of both the unlabeled and <sup>13</sup>C-labeled  
81 molecules are equal but shifted in mass. Hence, the method only requires the previous  
82 measurement of MID for the unlabeled compound. However, this classical correction  
83 overestimates <sup>13</sup>C natural abundance contributions when the number of C atoms in the  
84 molecule increases. To solve these problems, current corrections are based on computational  
85 methods that calculate theoretical MIDs of labeled isotopologues<sup>37-39</sup>. A second strategy,  
86 widely employed to calculate MID, is based in the least squares approach developed by  
87 Brauman<sup>40</sup> in 1966. In these methods multiple linear regression is employed to solve a system  
88 of linear equations in which the experimental abundances are related to the theoretical and  
89 fractional abundances of unlabeled and labeled isotopologues<sup>41-42</sup>. The mass spectra of the  
90 unlabeled compound is measured and used to calculate the theoretical mass spectra for the

91 different labeled isotopologues. The third strategy is based on the calculation of complete  
92 mass isotopologue distributions including positional isotopologues using different techniques:  
93 GC-MS<sup>43</sup>, GC-MS-MS and LC-MS-MS<sup>44-46</sup>. For example, a recent study based on tandem  
94 mass spectrometry and least-squares regression measured the complete isotopologue  
95 distribution of aspartate<sup>47</sup>. The theoretical tandem MS distribution of unlabeled and labeled  
96 aspartate was calculated using a binomial distribution using the natural and labeled isotopic  
97 abundances of all elements present in the molecule.

98

99 We present here an improved methodology for MID analysis of intracellular metabolites in  
100 cell lines cultures by multiple linear regression and GC-MS. The method is able to measure  
101 isotopologue molar fractions in twenty-eight intracellular metabolites derived from glucose  
102 metabolism. The proposed strategy was applied to study metabolic differences in normal and  
103 prostate cancer cell lines grown in the presence of 2-<sup>13</sup>C<sub>1</sub> glucose. The novelty of this  
104 methodology in comparison with previous published approaches relies on three main points:  
105 i) experimentally measured values of % <sup>13</sup>C enrichment of the labeled glucose are employed  
106 instead of using the value provided by the manufacturer, ii) the purity of the selected cluster  
107 for each metabolite is studied to calculate the contribution of either the lack of mass  
108 resolution of the mass spectrometer, or the existence of different fragmentation mechanism  
109 such as the loss or gain of hydrogen atoms in the EI source and iii) a full validation of the  
110 proposed method is carried out by the comparison of the calculated molar fractions not only  
111 with theoretical values obtained from gravimetrically prepared mixtures of isotopologues but  
112 also with experimental values obtained by GC-Combustion-IRMS based on <sup>13</sup>C/<sup>12</sup>C isotope  
113 ratio measurements. Although spectral interferences are easily corrected by high resolution  
114 mass spectrometers we demonstrate in this work that the proposed method is able to correct  
115 for spectral interferences using widespread GC-EI-MS instrumentation. Using the proposed

116 procedure we have been able to quantify the lowest validated values of  $^{13}\text{C}$  incorporation ever  
117 reported in the literature. Initial studies on the application of the procedure to study the  
118 glucose metabolism of different prostate cell lines are also presented.

## 119 **2. EXPERIMENTAL**

### 120 **2.1 REAGENTS AND MATERIALS**

121 Natural abundance D-glucose ( $\geq 99.5\%$ ), L-alanine ( $\geq 98\%$ ), glycine ( $\geq 98.5\%$ ),  $\beta$ -alanine ( $\geq$   
122  $99\%$ ), L-valine ( $\geq 98\%$ ), L-leucine ( $\geq 98\%$ ), L-isoleucine ( $\geq 98\%$ ), L-proline ( $\geq 99\%$ ), L-  
123 methionine ( $\geq 98\%$ ), L-serine ( $\geq 99\%$ ), L-threonine ( $\geq 98\%$ ), L-lysine ( $\geq 98\%$ ), tyrosine  
124 ( $\geq 98\%$ ), L-phenylalanine ( $\geq 98\%$ ), cysteine ( $\geq 97\%$ ), L-aspartic acid ( $\geq 98\%$ ), L-glutamic acid  
125 ( $\geq 99\%$ ), sodium fumarate dibasic ( $\geq 99\%$ ), D-ribulose-5-phosphate disodium salt ( $\geq 96\%$ ),  
126 sodium citrate tribasic dehydrate ( $\geq 99\%$ ), urea ( $95\%$ ), sodium succinate dibasic ( $\geq 98\%$ ),  
127 sodium L-lactate ( $98\%$ ), dodecanoic acid ( $98\%$ ), myristic acid ( $99\%$ ), palmitic acid ( $\geq 99\%$ ),  
128 stearic acid ( $\geq 98.5\%$ ), cholesterol ( $\geq 99\%$ ) were purchased from Sigma-Aldrich (St. Louis,  
129 MO, USA). Disodium DL-malate ( $\geq 98\%$ ) was purchased from Merck (Darmstadt,  
130 Germany). D-glucose-2- $^{13}\text{C}_1$ , D-glucose-1,2- $^{13}\text{C}_2$ , D-glucose-1,2,3- $^{13}\text{C}_3$ , D-glucose- $^{13}\text{C}_6$ ,  
131 glycine-2- $^{13}\text{C}_1$  and glycine- $^{13}\text{C}_2$  were also purchased from Sigma-Aldrich. For cell culture,  
132 we employed normal human prostate epithelium PNT1A cells (Cat Number # 95012614),  
133 androgen-sensitive human prostate adenocarcinoma LNCaP cells (Cat Number # CRL-1740),  
134 androgen-insensitive human prostate carcinoma PC3 cells (Cat Number # CRL-1435)  
135 obtained from “European Collection of Cell Cultures” (ECACC, Wiltshire, UK) and from  
136 “American Type Culture Collection” (ATCC, Rockville, MD). LNCaP<sup>S12</sup> cells (LNCaP cells  
137 transfected with expression vector pcDNA3 containing the human MnSOD cDNA) and  
138 LNCaP<sup>MOCK</sup> cells (LNCaP cells transfected with the corresponding empty vector) were  
139 developed in our laboratory. RPMI 1640 and DMEM/F12 medium were purchased from  
140 Lonza (Basel, Switzerland), fetal bovine serum was purchased from Gibco life Technologies

141 (Waltham, USA). L-glutamine, HEPES, penicillin, streptomycin, amphotericin B,  
142 Dulbecco's phosphate buffered saline were purchased from Sigma-Aldrich (St. Louis, MO,  
143 USA). Flask T75 was purchased from Corning (Corning NY, USA), and 60 mm dishes were  
144 purchased from DB (New Jersey, USA). Methoxyamine hydrochloride (98%), N-tert-  
145 butyldimethylsilyl-N-methyltrifluoroacetamide with 1% tert-butyldimethylchlorosilane  
146 ( $\geq 95\%$ ), pyridine ( $\geq 98\%$ ) and propionic anhydride ( $\geq 95\%$ ) was purchased from Sigma-  
147 Aldrich (St. Louis, MO, USA). Hydroxylamine hydrochloride ( $\geq 99\%$ ) was purchased from  
148 ACROS (Gael, Belgium). Methanol was purchased by Fischer-Scientific (Madrid, Spain),  
149 ethyl acetate and hexane was supplied by Merck (Darmstadt, Germany). Eppendorf tubes (1.5  
150 ml) were purchased from Labbox (Mataró, Spain) and ultrapure water was obtained from a  
151 Milli-Q system Millipore (Bedford, MA, USA).

152

## 153 **2.2 INSTRUMENTATION**

154 A gas chromatograph, Agilent 7890, coupled to a triple quadrupole mass spectrometer,  
155 Agilent 7000 Series Triple Quad GC/MS (Agilent Technologies, Wilmington, DE, USA)  
156 operating at 70 eV was employed. The GC was fitted with a split/splitless injector and a DB-  
157 5 MS capillary column (cross-linked 5% phenyl-methyl siloxane, 30 m x 0.25 mm i.d., 0.25  
158  $\mu\text{m}$  coating). In addition, a Trace GC Ultra chromatograph from Thermo (Bremen, Germany)  
159 equipped with a GC Triplus Autosampler, split/splitless injector, a GC-Isolink interface and  
160 a Conflo IV universal interface with a Ni/CuO/Pt combustion reactor set a 1000°C was  
161 employed coupled to a Delta V advantage sector field mass-spectrometer (Thermo). An  
162 analytical balance model AB204-S (Mettler Toledo, Zurich, Switzerland) was used for the  
163 gravimetric preparation of all solutions. A centrifuge 5810R D from Eppendorf (Hamburg,  
164 Germany) was used to remove debris. A centrifugal vacuum concentrator from Genevac  
165 (Sulflok, UK) was employed for sample evaporation. A thermomixer compact from

166 Eppendorf (Hamburg, Germany) was used to control the temperature of the derivatization  
167 reactions.

168

## 169 **2.3 PROCEDURES**

### 170 *2.3.1 Cell culture growth*

171 Normal human prostate epithelium PNT1A cells, androgen-sensitive human prostate  
172 adenocarcinoma LNCaP cells, androgen-insensitive human prostate carcinoma PC3 cells,  
173 LNCaP<sup>S12</sup> cells (LNCaP cells transfected with expression vector pcDNA3 containing the  
174 human MnSOD cDNA) and LNCaP<sup>MOCK</sup> cells (LNCaP cells transfected with the  
175 corresponding empty vector) were maintained in RPMI 1640, or DMEM/F12 medium  
176 supplemented with 10% Fetal Bovine Serum, 2 mM L-Glutamine, 15 mM HEPES and an  
177 antibiotic-antimycotic cocktail containing 100 U/ml penicillin, 10 µg/ml streptomycin and  
178 0.25 µg/ml amphotericin B. All cell lines were grown at 37°C in a humidified 5% CO<sub>2</sub>  
179 atmosphere. The medium was changed every 2 days and cultures were split at least once a  
180 week. Before each experiment, near-confluent cultures were harvested by brief trypsinization  
181 and seeded at a density of 25,000 cell/ml on 60 mm dishes and allowed to attach overnight  
182 before treatments. Then, media was replaced, cells were washed with DPBS and media with  
183 2g/L of 2-<sup>13</sup>C<sub>1</sub>-glucose were added during 24h. After treatments, cells were washed twice  
184 with ice-cold DPBS and harvested by cell scraping briefly at room temperature and pelleted  
185 by centrifugation at 500 g for 5 min at 4°C. Each sample was kept frozen at -80°C until  
186 processing.

187

### 188 *2.3.2 Extraction of intracellular metabolites*

189 Intracellular metabolites were extracted from cell pellets by a double extraction with 100%  
190 methanol at -80°C followed by a single extraction with milli-Q water<sup>48</sup>. The frozen pellet cells



191 were resuspended in 500  $\mu$ L of methanol at  $-80^{\circ}\text{C}$ , snap-frozen in liquid nitrogen and  
192 thawed in a mixture of liquid nitrogen-acetone to about  $-80^{\circ}\text{C}$ . After vortexing for 30 s and  
193 pelleting by centrifugation at 800g for 1 min, the supernatant was transferred to a fresh  
194 microcentrifuge tube on liquid nitrogen-acetone mixture at  $-80^{\circ}\text{C}$ . The pellet cells were again  
195 resuspended in 500  $\mu$ L of methanol at  $-80^{\circ}\text{C}$  and the freeze-thaw-vortex-pellet cycle was  
196 repeated. The supernatant was transferred and pooled with the previous methanol extract at -  
197  $80^{\circ}\text{C}$ . Finally, the cell pellet was resuspended in 250  $\mu$ L of milli-Q water, and the freeze-  
198 thaw cycle was repeated for a last time. The cells were then vortexed for 30s and pelleted by  
199 centrifugation at 15000g for 1 min. The supernatant was removed and pooled with the  
200 previously pooled methanol extracts. The pooled supernatant fractions were centrifuged at  
201 15000g for 1 min in order to remove cell debris. Then, the supernatant was transferred to a  
202 fresh tube using a Pasteur pipette and evaporated to dryness at  $30^{\circ}\text{C}$  in a centrifugal vacuum  
203 concentrator. Dried intracellular metabolites were kept at  $-80^{\circ}\text{C}$  prior derivatization and GC-  
204 MS analysis.

205

### 206 *2.3.3 Derivatization of intracellular metabolites*

207 The extracted metabolites were dissolved in 100 $\mu$ L of 2% methoxyamine hydrochloride in  
208 pyridine and incubated at  $40^{\circ}\text{C}$  for 8 min on a thermomixer compact. Next, 150 $\mu$ L of a  
209 mixture of N-tert-Butyldimethylsilyl-N-methyltrifluoroacetamide and 1% tert-  
210 Butyldimethylchlorosilane (TBDMCS) was added and the samples were incubated for 10 min  
211 at  $60^{\circ}\text{C}$ . The derivatized samples were centrifuged for 2 min at 14000 g to remove debris and  
212 the clear liquid was transferred into a GC vial for GC-MS analysis.

213

### 214 *2.3.4 Derivatization and GC-MS determination of glucose*

215 <sup>13</sup>C-labeling of glucose in the medium cell culture was determined by GC-MS analysis of the  
216 aldonitrile pentapropionate derivative of glucose. For this purpose, 100 μL of medium was  
217 evaporated to dryness at 30°C in a centrifugal vacuum concentrator. Next, 100 μL of  
218 hydroxylamine hydrochloride solution (20 mg/mL in pyridine) was added to the samples. The  
219 samples were incubated at 90°C for 8 min, followed by addition of 150 μL of propionic  
220 anhydride. After 10 min incubation at 60°C, the samples were evaporated to dryness at 50°C,  
221 dissolved in 100 μL of ethyl acetate and transferred into GC vials for GC-MS analysis.

222

### 223 *2.3.5 GC-MS experimental conditions for the separation and detection of intracellular* 224 *metabolites*

225 The column temperature was initially held at 60 °C for 1 min, and then a temperature ramp of  
226 5°C/min was applied until 320 °C for 10 min. The total run time was 68 min. Helium was  
227 used as a carrier gas at a flow rate of 2 mL/min. The injector temperature was kept at 250°C  
228 while the interface temperature and the ion source were 280°C and 230°C, respectively. A  
229 sample volume of 2 μL was injected in splitless mode with 1 min of purge time. The electron  
230 ionization source was operated at 70eV. A full fragment cluster for each metabolite was  
231 measured in SIM mode using 10ms of dwell time per mass.

232

### 233 *2.3.6 GC-MS experimental conditions for the separation and detection of glucose*

234 The injection volume was 2 μL and the samples were injected in splitless mode. GC oven  
235 temperature was held at 70°C for 2 min, increased to 300°C at 20°C/min, and held for 3 min.  
236 Mass isotopologue distribution of Glucose was determined from the cluster at m/z 370, which  
237 contains the C1-C5 carbon atoms of Glucose.

238

239 *2.3.7 GC-C-IRMS experimental conditions for intracellular metabolite- specific  $^{13}\text{C}/^{12}\text{C}$*   
240 *isotope ratio measurement*

241 For GC-C-IRMS analysis, 1  $\mu\text{L}$  of sample was injected in the splitless mode by an  
242 autosampler at 250°C. Helium was used as carrier gas at a flow rate of 2 mL/min. The energy  
243 applied at the EI source was 124 eV. Two Faraday cup collectors for m/z 44 and 45, were  
244 used for  $\text{CO}_2$  detection. Chromatographic conditions were the same as those employed in  
245 GC-MS analysis.  $^{13}\text{C}/^{12}\text{C}$  isotope ratio was calculated from the integrated areas of m/z 44 and  
246 m/z 45.

247

248 *2.3.8 GC-C-IRMS experimental conditions for glucose-specific  $^{13}\text{C}/^{12}\text{C}$  isotope ratio*  
249 *measurement*

250 1  $\mu\text{L}$  of sample was injected in split mode (1:5) at 250°C. The GC oven temperature was held  
251 at 70°C for 2 min, increased to 230°C at 20°C/min, at 10°C/min to 300°C and finally held for  
252 5 min. Glucose-specific  $^{13}\text{C}/^{12}\text{C}$  isotope ratio was calculated from the integrated peak areas of  
253 m/z 44 and m/z 45.

254

255 *2.3.9 Multiple linear regression for MID analysis*

256 For the measurement of the MID of the different intracellular metabolites, the experimental  
257 isotopic distribution measured by GC-MS can be assumed to be a linear combination of all  
258 possible isotopologues with a different incorporation of  $^{13}\text{C}$  in the molecule. The relative  
259 contribution of different isotope patterns in the experimental mass spectra can be calculated  
260 by multiple linear regression<sup>49</sup>. This is better described in equation (1) in matrix notation for  
261 the measurement of a given number of  $m$  masses in a compound  $a$ .

$$\begin{matrix} 262 \\ \end{matrix}
\begin{pmatrix} {}^a A_{sample}^1 \\ {}^a A_{sample}^2 \\ {}^a A_{sample}^3 \\ \vdots \\ {}^a A_{sample}^m \end{pmatrix} = \begin{pmatrix} {}^a A_{nat}^1 & {}^a A_{13C1}^1 & {}^a A_{13C2}^1 & {}^a A_{13C3}^1 & {}^a A_{13C4}^1 & \cdots & {}^a A_{13Cn}^1 \\ {}^a A_{nat}^2 & {}^a A_{13C1}^2 & {}^a A_{13C2}^2 & {}^a A_{13C3}^2 & {}^a A_{13C4}^2 & \cdots & {}^a A_{13Cn}^2 \\ {}^a A_{nat}^3 & {}^a A_{13C1}^3 & {}^a A_{13C2}^3 & {}^a A_{13C3}^3 & {}^a A_{13C4}^3 & \cdots & {}^a A_{13Cn}^3 \\ \vdots & \vdots & \vdots & \vdots & \vdots & \vdots & \vdots \\ {}^a A_{nat}^m & {}^a A_{13C1}^m & {}^a A_{13C2}^m & {}^a A_{13C3}^m & {}^a A_{13C4}^m & \cdots & {}^a A_{13Cn}^m \end{pmatrix} \cdot \begin{pmatrix} {}^a x_{nat} \\ {}^a x_{13C1} \\ {}^a x_{13C2} \\ {}^a x_{13C3} \\ {}^a x_{13C4} \\ \vdots \\ {}^a x_{13Cn} \end{pmatrix} + \begin{pmatrix} {}^a e^1 \\ {}^a e^2 \\ {}^a e^3 \\ \vdots \\ {}^a e^m \end{pmatrix} \quad (1)$$

263 Where  ${}^a A_{sample}^m$  refers to the experimental abundances measured by mass spectrometry in the  
264 sample and  ${}^a A_{nat}^m$  to the natural theoretical isotope abundances.  ${}^a A_{13C1}^m$  and  ${}^a A_{13Cn}^m$  are the  
265 theoretical isotope abundances calculated when one or  $n$  atoms of  $^{13}\text{C}$ , respectively are  
266 incorporated into the molecule. Theoretical isotope abundances are calculated with a visual  
267 basic program written as a macro for Microsoft Excel<sup>50-51</sup> by adapting the calculation  
268 algorithm described by Kubinyi<sup>52</sup>. IUPAC data on the natural isotopic composition of the  
269 elements, the exact mass of the isotopes and the exact value of  $^{13}\text{C}$  enrichment calculated  
270 experimentally<sup>53</sup> were introduced in the spreadsheet and were read from the visual basic  
271 program. Therefore, although the proposed procedure is not able to provide positional  
272 information (isotopomer analysis), it is able to correct for the contribution of other natural  
273 abundance elements such as Si. Finally,  ${}^a x_{13Cn}$  refers to the unknown molar fraction, which  
274 provides the contribution of the incorporation of  $n$  atoms of  $^{13}\text{C}$  in the molecule. As we have  
275 more parameters (nominal masses) than unknowns (molar fractions) an error vector  $e$  is  
276 included. The molar fractions can be obtained by multiple linear regression using  
277 conventional spreadsheet software (e.g. LINEST function of Microsoft Excel). Note that the  
278 theoretical abundances used in equation (1) will have to be corrected by spectral purity as  
279 discussed below.

### 280 3. RESULTS AND DISCUSSION

281

### 282 **3.1 Identification of the intracellular metabolites**

283 For the identification of the intracellular metabolites the samples were measured in SCAN  
284 mode and the experimental spectra were compared with Wiley and NIST MS libraries. Once  
285 the structure was proposed by the library, it was confirmed by injecting a natural abundance  
286 standard to compare the experimental mass spectra and the retention times. A total number of  
287 28 metabolites including 16 amino acids, 7 small metabolites including organic acids and 5  
288 fatty acids, including here cholesterol, were positively identified. Then, a full cluster for each  
289 metabolite was measured in SIM mode to calculate the isotopic distribution. The identity of  
290 the metabolite, the fragment formula and the measured cluster for each metabolite are given  
291 in Table 1. In all cases, the selected cluster contained the original number of C atoms of the  
292 underivatized molecule. Most of the clusters corresponded to the M-57 ion with the main in-  
293 source fragmentation being the loss of the tertbutyl group from the derivatizing reagent.

294

### 295 **3.2 Spectral purity of the selected clusters for each intracellular metabolite**

296 When using the EI source, different fragmentation mechanism may occur simultaneously<sup>53, 54</sup>  
297 generating spectral interferences which prevent the accurate measurement of the isotope  
298 patterns of the metabolites. First, fragment ions containing different numbers of hydrogen  
299 atoms can be obtained which overlap in the mass spectrum and secondly, the resolution of the  
300 mass spectrometer employed may not be adequate so that tailing of a given mass peak [*a*] at  
301 masses [*a*-1] could be observed even in a properly tuned and calibrated instrument<sup>53</sup>.  
302 Although the correction of these contributions may not be significant in metabolic flux  
303 analysis we decided to apply such correction to improve the accuracy and precision of the  
304 developed methodology. The contribution of the loss of hydrogen or the tailing of the peaks  
305 at the low mass side can be calculated simultaneously as the isotopic composition of the [*a*-  
306  $H^+$ ] ion is almost the same as that of the [*a*] ion but shifted one nominal mass unit. So, given

307 the main ion  $[a]$  of a given cluster, we can find spectral overlap with  $[a+H^+]$  or  $[a-H^+]$  ions,  
 308 so the purity of the selected cluster must be studied for accurate metabolic data to be obtained  
 309 in real samples. Such potential mass overlap can be quantified by comparing the  
 310 experimentally measured isotope abundances for the selected cluster of the natural abundance  
 311 compound with the theoretical abundances calculated for  $[a]$ ,  $[a+H^+]$ ,  $[a-H^+]$  and other  
 312 possible ions using equation (2)<sup>49,55</sup>.

313

$$\begin{bmatrix} A_{\text{exp}}^1 \\ A_{\text{exp}}^2 \\ A_{\text{exp}}^3 \\ \dots \\ A_{\text{exp}}^{n-1} \\ A_{\text{exp}}^n \end{bmatrix} = \begin{bmatrix} A_a^1 & A_{a-H}^1 & A_{a+H}^1 & \dots & A_{a\pm jH}^1 \\ A_a^2 & A_{a-H}^2 & A_{a+H}^2 & \dots & A_{a\pm jH}^2 \\ A_a^3 & A_{a-H}^3 & A_{a+H}^3 & \dots & A_{a\pm jH}^3 \\ \dots & \dots & \dots & \dots & \dots \\ A_a^{n-1} & A_{a-H}^{n-1} & A_{a+H}^{n-1} & \dots & A_{a\pm jH}^{n-1} \\ A_a^n & A_{a-H}^n & A_{a+H}^n & \dots & A_{a\pm jH}^n \end{bmatrix} \cdot \begin{bmatrix} X_a \\ X_{a-H} \\ X_{a+H} \\ \vdots \\ X_{a\pm jH} \end{bmatrix} + \begin{bmatrix} e^1 \\ e^2 \\ e^3 \\ \dots \\ e^{n-1} \\ e^n \end{bmatrix} \quad (2)$$

314

315 In equation (2)  $A_{\text{exp}}^i$  refers to the measured abundance of the isotopologue  $i$ ,  $A_a^i$  the  
 316 theoretical abundance of the isotopologue  $i$  in the cluster  $[a]$ ,  $A_{a+H}^i$  the theoretical abundance  
 317 of the isotopologue  $i$  in the cluster  $[a+H^+]$  and  $A_{a-H}^i$  the theoretical abundance of the  
 318 isotopologue  $i$  in the cluster  $[a-H^+]$ .

319 Experiments were performed at five different concentration levels for each metabolite to  
 320 check for concentration effects during fragmentation and no changes due to concentration  
 321 were detected. The average results and their standard deviations obtained for each identified  
 322 intracellular metabolite are given in Table 2. For most compounds, the major contribution  
 323 arose from the  $[a]$  ion whereas contributions due to the lack of resolution of the mass  
 324 spectrometer or the loss of hydrogen atoms,  $[a-H^+]$  and  $[a-2H^+]$ , or the gain of hydrogen  
 325 atoms,  $[a+H^+]$ , were lower than 1% in general. However, certain compounds presented  
 326 significant contributions such as L-lysine where the contribution of  $[a-H^+]$  was about 2%,  $\beta$ -  
 327 alanine where  $[a-2H^+]$  was about 3%, glycine where the contribution of  $[a+H^+]$  was about

328 2% and ribulose 5P where the contribution of  $[a+H^+]$  reached even 6%. It is worth noting  
329 that the  $[a+H^+]$  contribution in fatty acids increased with the number of carbon atoms.  
330 Cholesterol, included in this group, reached a value of 2.5 %. According to these results, we  
331 considered that these contributions were significant and had to be taken into account when  
332 calculating the theoretical isotope patterns to be employed in equation (1).

333

334

### 335 **3.3 Determination of the enrichment of the isotopically labeled compounds by GC-MS**

336 For the determination of the isotopic enrichment of the labeled standards we followed a  
337 procedure previously developed in our laboratory<sup>53</sup>. For this purpose, the measured isotope  
338 distribution of all labeled compounds was compared with theoretically derived distributions  
339 calculated for different tentative isotope enrichments. The isotope enrichment providing the  
340 minimum in the square sum of residuals for the linear regression between the theoretical and  
341 experimental spectra is selected as the true enrichment. The calculated isotopic enrichments  
342 obtained from n=5 independent GC-MS injections were 98.4% for D-Glucose-2-<sup>13</sup>C<sub>1</sub>, 98.9%  
343 for D-Glucose-1,2-<sup>13</sup>C<sub>2</sub>, 99.9% for D-Glucose-1,2,3-<sup>13</sup>C<sub>3</sub>, 99.0% for D-Glucose-<sup>13</sup>C<sub>6</sub>, 98.4%  
344 for Glycine-2-<sup>13</sup>C and 99.5% for Glycine-<sup>13</sup>C<sub>2</sub>. Note that, in most cases, the calculated  
345 isotopic enrichment is significantly different to the nominal value provided by the  
346 manufacturers (99%) and that this value is provided without any associated uncertainty. The  
347 calculated isotopic enrichments for <sup>13</sup>C in the different compounds were then used in the  
348 calculation of the theoretical isotopic distribution of the different isotopologues of the  
349 metabolites to improve the accuracy and precision of the MID analysis in real samples. The  
350 calculated isotope enrichments for three selected metabolites (glycine, serine and L-alanine)  
351 when using D-Glucose-2-<sup>13</sup>C<sub>1</sub> enriched at 98.4% are included both before (Table 3) and after  
352 (Table 4) the correction for spectral purity taking into account the results given in Table 2.

353 The values given in Table 4 were then employed in equation (1) for the calculation of the  
354 molar fraction of the different isotopologues when using D-Glucose-2-<sup>13</sup>C<sub>1</sub> in cell cultures.

355

### 356 **3.4 Validation of the methodology**

357 The proposed methodology was first validated with the analysis of gravimetrically prepared  
358 mixtures of natural abundance and labeled compounds. In this way, the experimental molar  
359 fractions obtained by equation (1) could be compared with theoretical molar fractions. We  
360 selected glucose and glycine as model compounds in the validation experiments. Glycine was  
361 chosen because it is involved in numerous processes of glucose metabolism and glucose was  
362 selected due to the specific sample preparation procedure applied. The derivatization  
363 procedure employed for the intracellular metabolites uses methoxyamine hydrochloride and  
364 N-tert-Butyldimethylsilyl-N-methyltrifluoroacetamide (MTBSTFA) whereas that employed  
365 for glucose is based on a derivatization with propionic acid anhydride. Details of both  
366 procedures are given in the experimental section. In this way we could evaluate our  
367 calculations with two different sample preparation procedures.

368

#### 369 *3.4.1 Analysis of gravimetrically prepared mixtures of natural abundance and labeled* 370 *glucose*

371 A first validation experiment was carried out analyzing ten mixtures containing natural  
372 abundance D-glucose, D-glucose-2-<sup>13</sup>C<sub>1</sub>, D-glucose-1,2-<sup>13</sup>C<sub>2</sub>, D-glucose-1,2,3-<sup>13</sup>C<sub>3</sub> and D-  
373 glucose-<sup>13</sup>C<sub>6</sub> prepared from solutions of known concentration. In all mixtures, the molar  
374 fraction (%) of natural abundance glucose was kept constant at a value of approximately 18-  
375 19% whereas the molar fractions of the different labeled analogues were modified between  
376 10 and 40%. It is interesting to note that the last four mixtures were prepared in the absence  
377 of one of the labeled analogues. The results obtained are given in Table 5. The uncertainty of



378 the experimental values corresponds to the standard deviation of three independent GC-MS  
379 determinations. The uncertainties of the theoretical molar fractions were calculated following  
380 the procedure proposed by Kragten<sup>56</sup> in which the uncertainty of the weight of the solutions,  
381 the purity of the solutions and the molecular weights of all glucose analogues was taken into  
382 account. Table 5 shows that there are no statistical differences between the theoretical and  
383 experimental molar fractions for each analogue in all prepared mixtures. Also, negligible  
384 molar fractions were obtained for those glucose analogues removed from the preparation of  
385 mixtures 7, 8, 9 and 10.

386

387 Although the real challenge in metabolic flux analysis is the trueness and precision of all  
388 isotopologue fractions we carried out additional validation experiments to identify the lowest  
389 value of <sup>13</sup>C incorporation that could be accurately calculated with the proposed  
390 methodology. For this purpose, we prepared eight quinary mixtures containing natural  
391 abundance glucose, D-glucose-2-<sup>13</sup>C<sub>1</sub>, D-glucose-1,2-<sup>13</sup>C<sub>2</sub>, D-glucose-1,2,3-<sup>13</sup>C<sub>3</sub> and D-  
392 glucose-<sup>13</sup>C<sub>6</sub>, in such a way that the molar fraction of each <sup>13</sup>C labeled analogue in the  
393 mixture ranged from 0.015 to 4%. Figure 1 shows the comparison between the theoretical and  
394 experimental values obtained for the molar fractions of each labeled analogues. As can be  
395 observed, all data agreed well with the expected values down to ca. 0.05% of labeled glucose.  
396 It is worth noting also that when using D-glucose-1,2,3-<sup>13</sup>C<sub>3</sub> and D-glucose-<sup>13</sup>C<sub>6</sub> all the  
397 experimental values obtained agreed well with the theoretical values. However, when using  
398 D-glucose-1,2-<sup>13</sup>C<sub>2</sub> and D-glucose-2-<sup>13</sup>C<sub>1</sub> we could not obtain accurate molar fractions for  
399 lowest isotope enrichments studied of 0.037% and 0.015%. These results suggest that the  
400 accuracy obtained for <sup>13</sup>C incorporation at this very low enrichment level may depend on the  
401 number of <sup>13</sup>C atoms of the labeled analogue.

402

403 Then, we studied the minimum molar fraction of the labeled glucose analogues which could  
404 be detected in binary mixtures by preparing a group of five mixtures containing natural  
405 glucose and D-glucose-2- $^{13}\text{C}_1$  and another group of five mixtures containing natural glucose  
406 and D-glucose- $^{13}\text{C}_6$ . In both groups the molar fraction of the labeled analogue was varied  
407 between 0.015 and 0.35%. Figure 2 shows the results obtained in both groups of mixtures. As  
408 can be observed the procedure provided accurate experimental values when the molar  
409 fraction was higher or equal to 0.07% for both labeled analogues. When using D-glucose-  
410  $^{13}\text{C}_6$ , the experimental molar fractions for values lower than 0.07% were much closer to the  
411 theoretical values than those obtained using D-glucose-2- $^{13}\text{C}_1$ . In addition, the standard  
412 deviation of the molar fraction obtained for 0.07% when using D-glucose- $^{13}\text{C}_6$  (0.002) was  
413 ten times lower than that obtained when using D-glucose-2- $^{13}\text{C}_1$  (0.022). These results  
414 demonstrate the influence of the number of  $^{13}\text{C}$  atoms not only on the accuracy but also on  
415 the precision of the molar fractions. Other procedures published in the literature were able to  
416 validate isotopologue molar fractions in the range of 1.7%<sup>42</sup> and 0.3%<sup>21</sup>. Therefore, our  
417 validated molar fractions of 0.07% are, to the best of our knowledge, the lowest validated  
418 molar fractions reported in the literature.

419

#### 420 *3.4.2 Analysis of gravimetrically prepared mixtures of natural abundance and labeled* 421 *glycine*

422 First we prepared a group of five binary mixtures containing natural glycine and glycine-2-  
423  $^{13}\text{C}_1$ , a second group of five binary mixtures containing natural glycine and glycine- $^{13}\text{C}_2$  and  
424 a third group of five ternary mixtures containing natural glycine, glycine-2- $^{13}\text{C}_1$  and glycine-  
425  $^{13}\text{C}_2$ . The molar fraction (%) of natural abundance glycine was modified from 20 to 99%, and  
426 the molar fractions of the labeled glycine analogues from 1 to 50%. Table 6 shows the results  
427 obtained in the three groups of samples. As can be observed, the results obtained for the

428 experimental molar fractions calculated by equation (1) were in agreement with the  
429 theoretical molar fractions for the whole range of molar fractions assayed.

430

431 Finally, and in order to study the minimum enrichment which can be accurately measured for  
432 glycine, we prepared a group of four binary mixtures of natural abundance glycine and  
433 glycine-2-<sup>13</sup>C<sub>1</sub> and another group of four binary mixtures of natural abundance glycine and  
434 glycine-<sup>13</sup>C<sub>2</sub> at enrichment levels between 0.1 and 0.7% for the labeled analogues. The results  
435 obtained are shown in Table 7. As can be observed, the method was not able to provide  
436 accurate molar fractions at levels lower than 0.7% for both mixtures. These results show that  
437 the lowest amount of <sup>13</sup>C incorporation detected in this intracellular metabolite was ten times  
438 higher than that obtained previously for glucose. A possible reason for this result is that the  
439 mass cluster measured for glucose was pure while the spectral purity of glycine (see Table 2)  
440 showed the presence of the [a+H<sup>+</sup>] ion with a contribution of about 2% with relatively high  
441 experimental uncertainty. Obviously, the uncertainty of the [a+H<sup>+</sup>] contribution translated  
442 into a similar uncertainty for the calculated molar fractions of, particularly, glycine-2-<sup>13</sup>C<sub>1</sub>.

443

#### 444 *3.4.3 Measurement of <sup>13</sup>C/<sup>12</sup>C ratio by GC-C-IRMS for validation of GC-MS results*

445 A second validation of the proposed GC-MS method was carried by measuring compound-  
446 specific <sup>13</sup>C/<sup>12</sup>C isotope ratios by GC-C-IRMS from the measured areas of m/z 44 and m/z 45  
447 resulting from the oxidation of the target compounds to CO<sub>2</sub>. To carry out the comparison,  
448 molar fractions obtained by GC-MS were transformed into <sup>13</sup>C/<sup>12</sup>C isotope ratios using  
449 equation (3).

450

451

452

453

454

455 
$$\frac{{}^{13}C}{{}^{12}C} = \frac{(1 \cdot Ab_{13C1}^{13C} + (n-1) \cdot Ab_{nat}^{13C}) \cdot X_{13C1} + (2 \cdot Ab_{13C2}^{13C} + (n-2) \cdot Ab_{nat}^{13C}) \cdot X_{13C2} + \dots + (m \cdot Ab_{13Cm}^{13C} + (n-m) \cdot Ab_{nat}^{13C}) \cdot X_{13Cm} + n \cdot Ab_{nat}^{13C} \cdot X_{nat}}{(1 \cdot Ab_{13C1}^{12C} + (n-1) \cdot Ab_{nat}^{12C}) \cdot X_{13C1} + (2 \cdot Ab_{13C2}^{12C} + (n-2) \cdot Ab_{nat}^{12C}) \cdot X_{13C2} + \dots + (m \cdot Ab_{13Cm}^{12C} + (n-m) \cdot Ab_{nat}^{12C}) \cdot X_{13Cm} + n \cdot Ab_{nat}^{12C} \cdot X_{nat}}$$

456

457

458

459

(3)

460 In this equation  $m$  refers to the number of carbon atoms of the compound;  $n$  refers to the  
461 number of carbon atoms of the derivatized compound;  $Ab_{13Ci}^{13C}$  is the  $^{13}C$  abundance in an  
462 analogue labeled in  $i$   $^{13}C$  atoms,  $Ab_{13Ci}^{12C}$  is the natural abundance for  $^{12}C$  in an analogue labeled  
463 in  $i$   $^{13}C$  atoms,  $Ab_{nat}^{13C}$  is the natural abundance for  $^{13}C$ ,  $Ab_{nat}^{12C}$  is the natural  $^{12}C$  abundance,  $X_{nat}$   
464 is the molar fraction of the natural abundance compound and  $X_{13Ci}$  is the molar fraction of an  
465 analogue labeled in  $i$   $^{13}C$  atoms.

466

467 First, we calculated for the ten mixtures of Table 5 containing natural abundance D-glucose,  
468 D-glucose-2- $^{13}C_1$ , D-glucose-1,2- $^{13}C_2$ , D-glucose-1,2,3- $^{13}C_3$  and D-glucose- $^{13}C_6$  the global  
469  $^{13}C/^{12}C$  isotope ratio. For this purpose we used the isotopic enrichment calculated as  
470 described previously<sup>53</sup> and the experimental molar fractions for each labeled analogue  
471 obtained by GC-MS and equation (1). Then the mixtures were injected in triplicate into the  
472 GC-C-IRMS system to measure the glucose-specific  $^{13}C/^{12}C$  isotope ratio. Figure 3 compares  
473 the  $^{13}C/^{12}C$  isotope ratio calculated from the molar fractions obtained by GC-MS with the  
474  $^{13}C/^{12}C$  isotope ratio measured by GC-C-IRMS. For the ten mixtures, the  $^{13}C/^{12}C$  isotope  
475 ratios calculated with equation (3) using the molar fractions measured by GC-MS were in  
476 perfect agreement with the experimental  $^{13}C/^{12}C$  isotope ratios measured by GC-C-IRMS.  
477 The uncertainty of the  $^{13}C/^{12}C$  isotope ratio measurement by GC-C-IRMS calculated from  
478 three independent injections and expressed as relative standard deviation (RSD%) ranged  
479 from 0.3 to 2.5%. The uncertainty of the  $^{13}C/^{12}C$  isotope ratio calculated using equation (3)  
480 was calculated applying the Kragten procedure<sup>56</sup>. In this way, combined uncertainties were  
481 calculated taking into account not only the uncertainty of the molar fractions calculated from  
482 three independent GC-MS injections but also the uncertainties of the isotopic abundances of  
483 the natural abundance carbon and isotopically enriched carbon. Using the Kragten<sup>56</sup>  
484 procedure the relative standard deviation (RSD%) of the  $^{13}C/^{12}C$  isotope ratio calculated

485 using equation (3) ranged from 0.9 to 1.2 % which are slightly lower than those obtained by  
486 GC-IR-MS. Such difference can be attributed to the better sensitivity obtained in the GC-MS  
487 system in SIM mode compared to that obtained by GC-C-IRMS in which the peak heights  
488 ranged from 240 to 800 mV for  $m/z$  44.

489 Secondly, we followed the same validation strategy in the analysis of cell cultures of different  
490 prostate cancer cell lines grown in the presence of 2- $^{13}\text{C}_1$ -glucose. For this purpose, cell  
491 cultures were treated as described in the experimental section and simultaneously injected by  
492 triplicate in the GC-MS and in the GC-C-IRMS systems. This validation was performed for  
493 four intracellular metabolites involved in glucose metabolism: serine, malate, L-aspartate and  
494 L-glutamate. These intracellular metabolites were chosen because it was possible to obtain  
495 for all four compounds baseline-resolved chromatographic peaks in the GC-C-IRMS system,  
496 which is essential for an accurate  $^{13}\text{C}/^{12}\text{C}$  ratio measurement. Again, the experimental molar  
497 fractions obtained by GC-MS and equation (1) were converted into  $^{13}\text{C}/^{12}\text{C}$  ratios using  
498 equation (3) and compared with the  $^{13}\text{C}/^{12}\text{C}$  ratios directly measured by GC-C-IRMS. Table 8  
499 shows the molar fractions obtained for each labeled analogue and the resulting  $^{13}\text{C}/^{12}\text{C}$  ratios.  
500 As can be observed, for all four compounds and all four cell lines  $^{13}\text{C}/^{12}\text{C}$  isotope ratios  
501 calculated with equations (1) and (3) using the isotopic distributions measured by GC-MS  
502 were in perfect agreement with the experimental  $^{13}\text{C}/^{12}\text{C}$  isotope ratio measured by GC-C-  
503 IRMS. In this case, the uncertainty of the  $^{13}\text{C}/^{12}\text{C}$  isotope ratio measurement by GC-C-IRMS  
504 calculated from three independent injections and expressed as relative standard deviation  
505 (RSD%) ranged from 1.1 to 8.3% whereas that obtained by equations (1) and (3) and GC-MS  
506 ranged from 3.4 to 16.5%. An uncertainty budget for the measurement of the  $^{13}\text{C}/^{12}\text{C}$  isotope  
507 ratio of serine in PNT1A cell line calculated from the molar fractions obtained by GC-MS  
508 and equation (3) is given in Table 9. As can be observed the main contributor to the  
509 uncertainty is the uncertainty of the natural abundance  $^{13}\text{C}$ .

510

511 **3.5 Application to the measurement of mass isotopologue distributions in cultures of**  
512 **prostate cancer cell lines.**

513 To demonstrate the potential application of the proposed methodology we measured the mass  
514 isotopologue distributions of the twenty-eight intracellular metabolites in cultures of normal  
515 human prostate epithelium PNT1A cells and four different prostate cancer cell lines: PC3  
516 (androgen-insensitive human prostate carcinoma) LNCaP (androgen-sensitive human prostate  
517 adenocarcinoma) LNCaP<sup>S12</sup> (LNCaP cells transfected with expression vector pcDNA3  
518 containing the human MnSOD cDNA) and LNCaP<sup>MOCK</sup> (LNCaP cells transfected with the  
519 corresponding empty vector). Cells were grown in the presence of 2-<sup>13</sup>C<sub>1</sub>-glucose during 24h  
520 as described in the experimental section. <sup>13</sup>C incorporation was observed in sixteen of the  
521 twenty-eight metabolites studied. However, only L-alanine, glycine, serine, fumarate and  
522 succinate showed significant differences in <sup>13</sup>C labeling between the different cell lines. The  
523 actual mass isotopologue distributions measured by GC-MS for glycine, serine and L-alanine  
524 are given in Table 10 (average values for five determinations). From that data, and the data  
525 shown in Table 4, the molar fractions from the incorporation of <sup>13</sup>C in the different  
526 metabolites can be calculated. Figure 4 shows the molar fractions obtained for the <sup>13</sup>C<sub>1</sub>-  
527 analogue of L-alanine, glycine and serine in the different cell lines. As can be observed,  
528 PNT1A and PC3 cell lines showed negligible <sup>13</sup>C incorporation in glycine whereas the molar  
529 fraction for the serine <sup>13</sup>C<sub>1</sub>-analogue was lower than 3% in these two cell lines. However,  
530 when analyzing cultures of LNCaP, LNCaP<sup>S12</sup>, and LNCaP<sup>MOCK</sup> significant molar fractions  
531 of the <sup>13</sup>C<sub>1</sub>-analogue were detected in glycine (close to 10%) and in serine (between 10 and  
532 15%). In the same graph we plotted for comparison the results for L-alanine which showed a  
533 high and similar incorporation in all cell lines (between 25 and 35% enrichment).

534

535 Previous works have shown that the tumor suppressor protein p53 not only upregulates  
536 metabolic targets to inhibit tumorigenesis but also regulates glycolysis and oxidative  
537 phosphorylation<sup>57</sup>. More recently, it was demonstrated that serine starvation activates p53 to  
538 reprogram metabolism and increase cancer cell survival<sup>58</sup>. After glucose is converted into 3-  
539 phosphoglycerate through glycolysis and shuttled into the serine synthesis pathway, serine is  
540 converted into glycine, where p53 is elevated and activates p21 to promote cell-cycle arrest  
541 and replenish GSH (glutathione). In this way, conversion to inosine monophosphate (IMP)  
542 and resultant purine biosynthesis is suppressed and GSH pools suppress reactive oxygen  
543 species (ROS) generated from the TCA cycle<sup>58,59</sup>. According to this, we should observe a  
544 lower glycine production in cells lacking p53 activity (non-functional p53) as they generate  
545 IMP instead of replenishing the GMP pools. Similarly, a higher <sup>13</sup>C incorporation should be  
546 observed in p53<sup>+/+</sup> as glycine and subsequent GSH production is promoted. Figure 4 shows  
547 that our results are in agreement with this explanation as PNT1A and PC3 cell lines have  
548 non-functional p53 whereas LNCaP, LNCaP<sup>MOCK</sup>, LNCaP<sup>S12</sup> are p53<sup>+/+</sup> (functional p53 gen  
549 and protein).

550

#### 551 **4. CONCLUSIONS**

552 This work proposes an improved method for accurate and precise determinations of mass  
553 isotopologue distributions in intracellular glucose metabolites in cultures of prostate cancer  
554 cell lines. Three main aspects justify the novelty of the proposed procedure. First, theoretical  
555 isotopic distributions of the different isotopologues are previously calculated using an  
556 experimentally measured value of <sup>13</sup>C enrichment of the substrate (labeled glucose  
557 administrated to the cell cultures). Secondly, the purity of the selected cluster obtained for  
558 each compound in the GC-MS system used in this work is studied to calculate the  
559 contribution of different fragmentation mechanism such as the loss or gain of hydrogen atoms



560 in the EI source or the lack of resolution of the mass spectrometer. Using the experimental  
561 value for the glucose isotopic enrichment and the correction of the spectral purity of  
562 theoretical isotopic patterns of the intracellular metabolites the proposed procedure is able to  
563 correct for systematic errors which are not corrected in previous approaches and improves the  
564 accuracy and precision of the final molar fractions obtained from equation (1). The  
565 comparison with theoretical values obtained from gravimetrically prepared mixtures of  
566 different labeled analogues and with experimental values obtained by GC-C-IRMS based on  
567  $^{13}\text{C}/^{12}\text{C}$  isotope ratio measurements demonstrates the satisfactory accuracy and precision of  
568 the proposed procedure. Our results show that the spectral purity of the measured cluster and  
569 the number of  $^{13}\text{C}$  atoms of the labeled analogue strongly affect the minimum value of  $^{13}\text{C}$   
570 incorporation that can be accurately quantified. Using our experimental conditions the  
571 proposed procedure was able to accurately quantify in gravimetrically prepared mixtures of  
572 natural and labeled glucose molar fractions of 0.07% in binary and quinary mixtures. Those  
573 values are the lowest validated molar fractions reported in the literature. In addition, we have  
574 shown that the method is able to discriminate between different glucose metabolic routes in  
575 prostate cancer cell lines.

576

## 577 **5. ACKNOWLEDGEMENTS**

578 The authors are grateful for financial support from the Spanish Ministry of Economy and  
579 Competitiveness through Project Ref. CTQ2012-36711, co-funded by FEDER. The EU is  
580 acknowledged for the provision of FEDER funds for the purchase of the GC-MS/MS  
581 instrument. MFF acknowledges Gobierno del Principado de Asturias through Ficyt  
582 (Fundación para el Fomento en Asturias de la Investigación Científica Aplicada y la  
583 Tecnología) for the provision of a predoctoral grant in the frame of the Severo Ochoa  
584 Program (BP11-162).

585

586 **6. REFERENCES**

- 587 [1] O. Warburg, Über den stoffwechsel der carcinomzelle, *Biochem. Zeitschr.* 152 (1924)  
588 309-344.
- 589 [2] L. Galluzi, O. Keep, M.G. Vander Heiden, G. Kroemer, Metabolic targets for cancer  
590 therapy, *Nature Reviews.* 12 (2013) 829-846.
- 591 [3] R.J. De Berardinis, J.J. Lum, G. Hatzivassiliu, C.B. Thompson, The Biology of Cancer:  
592 Metabolic Reprogramming Fuels Cell Growth and Proliferation, *Cell metabolism.* 7 (2008)  
593 11-20.
- 594 [4] S.J. Barfeld, H.M. Itkonen, A. Urbanucci, I.G. Mills, Androgen-regulated metabolism and  
595 biosynthesis in prostate cancer, *Endocrine-Related Cancer.* 21 (2014) 57-66.
- 596 [5] D.J. Creek, A. Chokkathukalam, A. Jankevics, K.E.V. Burgess, R. Breitling, M.P. Barrett,  
597 Stable isotope-assisted metabolomics for network-wide metabolic pathway elucidation, *Anal.*  
598 *Chem.* 84 (2012) 8442-8447.
- 599 [6] A.N. Lane, T.W.N. Fan, R.M. Higashi, Stable isotope- assisted metabolomics in cancer  
600 research, *Life.* 60 (2008) 124-129.
- 601 [7] R. Schoenheimer, S. Ratner, D. Rittenberg, Studies in protein metabolism, *J. Biol.*  
602 *Chem.* 130 (1939) 703-732.
- 603 [8] R. Schoenheimer, D. Rittenberg, Deuterium as an indicator in the study of intermediary  
604 metabolism: The role of fat tissue, *J. Biol. Chem.* 111 (1935) 175-181.
- 605 [9] W. Washburn, H.C. Urey, Concentration of the H<sub>2</sub> Isotope of Hydrogen by the Fractional  
606 Electrolysis of Water, *Proc. N. A. S.* 18 (1932) 496-498.
- 607 [10] H.C. Urey, J.R. Huffman, H.G. Thode, M. Fox, Concentration of N<sup>15</sup> by Chemical  
608 Methods, *J. Chem. Phys.* 5 (1937) 856-867.
- 609 [11] H. Spencer, R. Eisinger, D. Laszlo, Metabolic and radioactive tracer studies in  
610 carcinoma of the prostate, *Am. J. Cancer. Res.* 29 (1960) 282-296.
- 611 [12] C.H. Wang, I. Stern, C.M. Gilmour, S. Klungsoyr, J.J. Braly, B.E. Christensen, V.H.  
612 Cheldelin, Comparative study of glucose catabolism by the radiorespirometric method, *J.*  
613 *Bacteriol.* 76 (1958) 207-216.
- 614 [13] J.L. Brazier, B. Ribon, M. Desage, B. Salle, Study of theophylline metabolism in  
615 premature human newborns using stable isotope labelling, *Biomed. Mass. Spectrom.* 7 (1980)  
616 189-192.

617 [14] J. U. Leonard, S.J.R. Heales, The investigation of inborn errors in vivo using stable  
618 isotopes, *Eur. J. Pediatrics*. 153 (1994) S81-S93.

619 [15] D. M. Bier, K.J. Arnold, W.R. Sherman, W.H. Holland, W.F. Holmes, D.M. Kipnis, In-  
620 vivo Measurement of Glucose and Alanine Metabolism with Stable Isotopic Tracers,  
621 *Diabetes*. 26 (1977) 1005-1015.

622 [16] J.K.H Tang, L. You, R.E. Blankenship, Y.J. Tang, Recent advances in mapping  
623 environmental microbial metabolisms through <sup>13</sup>C isotopic fingerprints, *J. R. Soc. Interface*. 9  
624 (2012) 2767-2780.

625 [17] I. W. Bogoard, T.S. Lin, J.C. Liao, Synthetic non-oxidative glycolysis enables complete  
626 carbon conservation, *Nature*. 502 (2013) 693-697.

627 [18] C.M. Metallo, M.G. Vander Heiden, Understanding metabolic regulation and its  
628 influence on cell physiology, *Mol. Cell*. 49 (2013) 388-398.

629 [19] S. Iwatani, S. Van Dien, K. Shimbo, K. Kubota, N. Kageyama, D. Iwahata, H. Miyano,  
630 K. Hirayama, Y. Usuda, K. Shimizu, K. Matsui, Determination of metabolic flux changes  
631 during fed-batch cultivation from measurements of intracellular amino acids by LC-MS/MS,  
632 *J. Biotechnol*. 128 (2007) 93-111.

633 [20] M.R. Antoniewicz, J.K. Keheller, G. Stephanopoulos, Accurate assessment of amino  
634 acid mass isotopologue distributions for metabolic flux analysis, *Anal. Chem*. 79 (2007)  
635 7554-7559.

636 [21] M.R. Antoniewicz, J.K. Keheller, G. Stephanopoulos, Measuring Deuterium Enrichment  
637 of Glucose Hydrogen Atoms by Gas Chromatography/Mass Spectrometry, *Anal. Chem*. 83  
638 (2011) 3211-3216.

639 [22] C. Cipollina, A. Ten Pierick, A.B. Canelas, R.M. Seifar, A.J.A. Van Maris, J.C. Van  
640 Dam, J.J. Heijnen, A comprehensive method for the quantification of the non-oxidative  
641 pentose phosphate pathway intermediates in *Saccharomyces cerevisiae* by GC-IDMS, *J.*  
642 *Chromatogr. B*. 877 (2009) 3231-3236.

643 [23] M. Koubaa, S. Mghaieth, B. Thomasset, A. Roscher, Gas chromatography-mass  
644 spectrometry analysis of <sup>13</sup>C labeling in sugars for metabolic flux analysis, *Anal. Biochem*.  
645 45 (2012) 183-188.

646 [24] R.W Leighty, M.R. Antoniewicz, Parallel labeling experiments with [U-<sup>13</sup>C] glucose  
647 validate *E. coli* metabolic network model for <sup>13</sup>C metabolic flux analysis, *Metab. Eng.* 14  
648 (2012) 533-541.

649 [25] J.C. Chatman, B. Bouchard, C. Des Rosiers, A comparison between NMR and GCMS  
650 <sup>13</sup>C-isotopologue analysis in cardiac metabolism, *Mol. Cell. Biochem*. 249 (2003) 105-112.

651 [26] R.J. Kleijn, J.M. Geertman, B.K. Nfor, C. Ras, D. Schipper, J.T. Pronk, J.J. Heijnen, A.J.  
652 Van Maris, W.A. Van Winden, Metabolic flux analysis of a glycerol-overproducing  
653 *Saccharomyces cerevisiae* strain based on GC-MS, LC-MS and NMR-derived <sup>13</sup>C-labelling  
654 data, *FEM. Yeast. Res.* 7 (2007) 216-231.

655 [27] J. Choi, M.R. Antoniewicz, Tandem mass spectrometry: a novel approach for metabolic  
656 flux analysis, *Metab. Eng.* 13 (2011), 225-233.

657 [28] Y. Yuan, T.M. Yang, E. Heinzle, <sup>13</sup>C metabolic flux analysis for larger scale  
658 cultivation using gas chromatography-combustion-isotope ratio mass spectrometry, *Meta.*  
659 *Eng.* 12 (2010) 392-400.

660 [29] W.S. Ahn, M.R. Antoniewicz, Metabolic flux analysis of CHO cells at growth and non-  
661 growth phases using isotopic tracers and mass spectrometry, *Meta. Eng.* 13 (2011) 598-609.

662 [30] L. Di Donato, C. Des Rosiers, J.A. Montgomery, F. David, M. Garneau, H.J.  
663 Brunengraber, Rates of gluconeogenesis and citric acid cycle in perfused livers, assessed  
664 from the mass spectrometric assay of the <sup>13</sup>C labeling pattern of glutamate, *Biol. Chem.* 268  
665 (1993) 4170-4180.

666 [31] C. Des Rosiers, L. Di Donato, B. Comte, A. Laplante, C. Marcoux, F. David, C.A.  
667 Fernandez, H. Brunengraber, Isotopologue analysis of citric acid cycle and gluconeogenesis  
668 in rat liver. Reversibility of isocitrate dehydrogenase and involvement of ATP-citrate lyase in  
669 gluconeogenesis, *J. Biol. Chem.* 270 (1995) 10027-10036.

670 [32] J. Katz, P. Wals, W.N. Paul-Lee, Isotopologue studies of gluconeogenesis and the Krebs  
671 cycle with <sup>13</sup>C-labeled lactate, *J. Biol. Chem.* 268 (1993) 25509-25521.

672 [33] J.C. Chatham, B. Bouchard, C. Des Rosiers, A comparison between NMR and GCMS  
673 <sup>13</sup>C-isotopologue analysis in cardiac metabolism, *Mol. Cell. Biochem.* 249 (2003) 105-112.

674 [34] J.Y. Jung, M.K. Oh, Isotope labeling pattern study of central carbon metabolites using  
675 GC/MS, *J. Chromatogr. B.* 974 (2015)101-108.

676 [35] T.H. Yang, C.J. Bolten, M.V. Coppi, J. Sun, E. Heinzle, Numerical bias estimation for  
677 mass spectrometric mass isotopologue analysis, *Anal. Biochem.* 388 (2009) 192-203.

678 [36] K. Biemann, *Mass Spectrometry*, McGraw-Hill, New York, 1962.

679 [37] C.A. Fernandez, C. Des Rosiers, S.F. Previs, Correction of <sup>13</sup>C mass isotopologue  
680 distributions for natural stable isotope abundance, *J. Mass. Spectrom.* 31 (1996) 255-262

681 [38] C. Des Rosiers, J.A. Montgomery, S. Desrochers, M. Garneau, O.A. Mamer, H.  
682 Brunengraber, Interference of 3-hydroxyisobutyrate with measurements of ketone body  
683 concentration and isotopic enrichment by gas chromatography-mass spectrometry, *Anal.*  
684 *Biochem.* 173 (1988) 96-105.

685 [39] T. Mairinger, M. Steiger, J. Nocon, D. Mattanovich, G. Koellensperger, S. Hann, Gas  
686 Chromatography-Quadrupole Time-of-Flight Mass Spectrometry-Based Determination of  
687 Isotopologue and Tandem Mass Isotopomer Fractions of Primary Metabolites for  
688  $^{13}\text{C}$ - Metabolic Flux Analysis, *Anal. Chem.* 87 (2015) 11792-11802.

689 [40] J.I. Brauman, Least squares analysis and simplification of multi-isotope mass spectra,  
690 *Anal. Chem.* 38 (1966) 607-610.

691 [41] W.N. Paul Lee, L.O. Byerley, E.A. Bergner, Mass isotopologue analysis: theoretical and  
692 practical considerations, *Biol. Mass. Spectrom.* 20 (1991) 451-458.

693 [42] M.E. Jennings, D.E. Matthews, Determination of complex isotopologue patterns in  
694 isotopically labeled compounds by mass spectrometry, *Anal. Chem.* 77 (2005) 6435-6444.

695 [43] B. Christensen, J. Nielsen, Isotopologue analysis using GC-MS, *Meta. Eng.* 1 (1999)  
696 282-290.

697 [44] P. Kiefer, C. Nicolas, F. Letisse, J.C. Portais, Determination of carbon labeling  
698 distribution of intracellular metabolites from single fragment ions by ion chromatography  
699 tandem mass spectrometry, *Anal. Biochem.* 360 (2007) 182-188.

700 [45] M.H. Jeffrey, J.W. Roach, C.J. Storey, D. Sherry, C.R. Malloy,  $^{13}\text{C}$  isotopologue  
701 analysis of glutamate by tandem mass spectrometry, *Anal. Biochem.* 300 (2002) 192-195.

702 [46] M. Rühl, B. Rupp, K. Nöh, W. Wiechert, W. Sauer, N. Zamboni, Collisional  
703 fragmentation of central carbon metabolites in LC- MS/MS increases precision of  $^{13}\text{C}$   
704 metabolic flux analysis, *Biotechnol. Bioeng.* 109 (2011) 763-771.

705 [47] J. Choi, M.T. Grossbach, M.R. Antoniewicz, Measuring complete isotopologue  
706 distribution of aspartate using gas chromatography/tandem mass spectrometry, *Anal. Chem.*  
707 84 (2012) 4628-4632.

708 [48] C.A. Sellick, R. Hansen, G.M. Stephens, R. Goodacre, A.J. Dickson, Metabolite  
709 extraction from suspension-cultured mammalian cells for global metabolite profiling, *Nat.*  
710 *Protoc.* 6 (2011) 1241-1249.

711 [49] J.I. García Alonso, P. Rodríguez-González, *Isotope Dilution Mass Spectrometry*, Royal  
712 Society of Chemistry, Cambridge (UK) 2013.

713 [50] J.I. García-Alonso, P. Rodríguez-González, A. González-Gago, A. González-Antuña,  
714 Determination of the uncertainties in the theoretical mass isotopologue distribution of  
715 molecules, *Anal. Chim. Acta.* 664 (2010) 68-76.

716 [51] J.I. Garcia-Alonso, P. Rodriguez-González, Response to “Comments on the uncertainties  
717 in isotope patterns of molecules” by J. Meija and Z. Mester (doi: 10.1016/j. aca. 2010.09.  
718 029), *Anal. Chim. Acta.* 694 (2011) 177-180.

719 [52] H. Kubinyi, Calculation of isotope distributions in mass spectrometry. A trivial solution  
720 for a non-trivial problem, *Anal. Chim. Acta.* 247 (1991) 107-119.

721 [53] A. González-Antuña, P. Rodríguez-González, J.I. García Alonso, Determination of the  
722 enrichment of isotopically labelled molecules by mass spectrometry, *J. Mass Spectrom.* 49  
723 (2014) 681-691.

724 [54] J. Mejia, J.A. Caruso, Deconvolution of isobaric interferences in mass spectra, *J. Am.*  
725 *Soc. Mass. Spectrum.* 15 (2004) 654-658.

726 [55] A. González-Antuña, P. Rodríguez-González, G. Centineo, J.I. García Alonso,  
727 Evaluation of minimal <sup>13</sup>C-labelling for stable isotope dilution in organic analysis, *Analyst.*  
728 135 (2010) 953-964.

729 [56] J. Kragten, Tutorial review. Calculating standard deviations and confidence intervals  
730 with a universally applicable spreadsheet technique, *Analyst.* 119 (1994) 2161-2165.

731 [57] E. Gottlieb, K.H. Vousden, p53 regulation of metabolic pathways, *Cold Spring Harb.*  
732 *Perspect. Biol.* 2 (2010) a001040.

733 [58] O.D. Maddocks, C.R. Berkers, S.M. Mason, L. Zheng, K. Blyth, E. Gottlieb, K.H.  
734 Vousden, *Nature.* 493 (2013) 542-546

735 [59] O. Tavan, W. Gu, The Hunger Games: p53 regulates metabolism upon serine starvation,  
736 *Cell Metabolism.* 17 (2013) 159-161.

737

738

739

740

741

742

743

744

745

746

747

748

749 **TABLES**

750 **Table 1.** Identity, fragment ion formula and m/z range measured by GC-MS in SIM mode for all the  
 751 intracellular metabolites identified in this work.

Metabolite	Selected in-source fragment ion formula	Measured cluster (m/z)
<b>Aminoacids</b>		
L-Proline	C <sub>13</sub> H <sub>28</sub> NO <sub>2</sub> Si <sub>2</sub>	284-293
L-Methionine	C <sub>13</sub> H <sub>30</sub> NO <sub>2</sub> Si <sub>2</sub> S	318-327
L-Lysine	C <sub>20</sub> H <sub>47</sub> N <sub>2</sub> O <sub>2</sub> Si <sub>3</sub>	429-438
L-Cysteine	C <sub>17</sub> H <sub>40</sub> NO <sub>2</sub> Si <sub>3</sub> S	404-413
L-Tyrosine	C <sub>23</sub> H <sub>44</sub> NO <sub>3</sub> Si <sub>3</sub>	464-476
L-Glutamate	C <sub>19</sub> H <sub>42</sub> NO <sub>4</sub> Si <sub>3</sub>	430-439
L-Valine	C <sub>13</sub> H <sub>30</sub> NO <sub>2</sub> Si <sub>2</sub>	286-295
L-Aspartate	C <sub>18</sub> H <sub>40</sub> NO <sub>4</sub> Si <sub>3</sub>	416-425
L-Leucine	C <sub>14</sub> H <sub>32</sub> NO <sub>2</sub> Si <sub>2</sub>	300-309
L-Isoleucine	C <sub>14</sub> H <sub>32</sub> NO <sub>2</sub> Si <sub>2</sub>	300-309
L-Phenylalanine	C <sub>17</sub> H <sub>30</sub> NO <sub>2</sub> Si <sub>2</sub>	334-346
Glycine	C <sub>10</sub> H <sub>24</sub> NO <sub>2</sub> Si <sub>2</sub>	244-253
L-Serine	C <sub>17</sub> H <sub>40</sub> NO <sub>3</sub> Si <sub>3</sub>	388-397
L-Threonine	C <sub>18</sub> H <sub>42</sub> NO <sub>3</sub> Si <sub>3</sub>	402-411
L-Alanine	C <sub>11</sub> H <sub>26</sub> NO <sub>2</sub> Si <sub>2</sub>	258-267
β-Alanine	C <sub>11</sub> H <sub>26</sub> NO <sub>2</sub> Si <sub>2</sub>	258-267
<b>Small metabolites</b>		
Urea	C <sub>9</sub> H <sub>23</sub> N <sub>2</sub> O <sub>2</sub> Si <sub>2</sub>	229-238
Succinate	C <sub>12</sub> H <sub>25</sub> O <sub>4</sub> Si <sub>2</sub>	287-296
Fumarate	C <sub>12</sub> H <sub>23</sub> O <sub>4</sub> Si <sub>2</sub>	285-294
Malate	C <sub>18</sub> H <sub>39</sub> O <sub>5</sub> Si <sub>3</sub>	417-426
Citrate	C <sub>20</sub> H <sub>39</sub> O <sub>6</sub> Si <sub>3</sub>	457-466
Lactate	C <sub>11</sub> H <sub>25</sub> O <sub>3</sub> Si <sub>2</sub>	259-268
Ribulose 5P	C <sub>13</sub> H <sub>28</sub> O <sub>7</sub> Si <sub>2</sub> P	381-390
<b>Fatty acids</b>		
Lauric acid	C <sub>14</sub> H <sub>29</sub> O <sub>2</sub> Si	255-264
Myristic acid	C <sub>16</sub> H <sub>33</sub> O <sub>2</sub> Si	283-292
Palmitic acid	C <sub>18</sub> H <sub>37</sub> O <sub>2</sub> Si	311-320
Stearic acid	C <sub>20</sub> H <sub>41</sub> O <sub>2</sub> Si	339-348
Cholesterol	C <sub>29</sub> H <sub>51</sub> O <sub>2</sub> Si	441-450

752

753

754

755

756

757 **Table 2.** Spectral purity of the selected clusters for the identified intracellular metabolites in the  
 758 electron ionization source (EI).

Metabolite	Molecular range of cluster (m/z)	Fragment formula	X <sub>M+</sub>	X <sub>M-H+</sub>	X <sub>M-2H+</sub>	X <sub>M+H+</sub>
<b>Aminoacids</b>						
L-Proline	284-293	C <sub>13</sub> H <sub>28</sub> NO <sub>2</sub> Si <sub>2</sub>	99.35±0.20	0.29±0.03	0.55±0.08	-----
L-Methionine	318-327	C <sub>13</sub> H <sub>30</sub> NO <sub>2</sub> Si <sub>2</sub> S	99.84±0.08	0.13±0.01	0.21±0.01	-----
L-Lysine	429-438	C <sub>20</sub> H <sub>47</sub> N <sub>2</sub> O <sub>2</sub> Si <sub>3</sub>	97.56±0.06	1.76±0.04	0.68±0.11	-----
L-Cysteine	404-413	C <sub>17</sub> H <sub>40</sub> NO <sub>2</sub> Si <sub>3</sub> S	100.05±0.02	-----	-----	-----
L-Tyrosine	464-476	C <sub>23</sub> H <sub>44</sub> NO <sub>3</sub> Si <sub>3</sub>	99.56±0.05	0.16±0.01	0.44±0.08	-----
L-Glutamate	430-439	C <sub>19</sub> H <sub>42</sub> NO <sub>4</sub> Si <sub>3</sub>	99.55±0.31	0.09±0.01	0.16±0.01	-----
L-Valine	286-295	C <sub>13</sub> H <sub>30</sub> NO <sub>2</sub> Si <sub>2</sub>	99.21±0.07	0.45±0.13	0.17±0.02	-----
L-Aspartate	416-425	C <sub>18</sub> H <sub>40</sub> NO <sub>4</sub> Si <sub>3</sub>	99.46±0.27	0.21±0.02	0.26±0.07	-----
L-Leucine	300-309	C <sub>14</sub> H <sub>32</sub> NO <sub>2</sub> Si <sub>2</sub>	99.14±0.14	0.22±0.02	0.20±0.03	0.24±0.04
L-Isoleucine	300-309	C <sub>14</sub> H <sub>32</sub> NO <sub>2</sub> Si <sub>2</sub>	99.45±0.05	0.22±0.01	0.13±0.01	0.18±0.06
L-Phenylalanine	334-346	C <sub>17</sub> H <sub>30</sub> NO <sub>2</sub> Si <sub>2</sub>	99.43±0.19	0.19±0.02	0.26±0.03	-----
Glycine	244-253	C <sub>10</sub> H <sub>24</sub> NO <sub>2</sub> Si <sub>2</sub>	97.59±0.57	0.49±0.04	0.12±0.02	1.70±0.42
L-Serine	388-397	C <sub>17</sub> H <sub>40</sub> NO <sub>3</sub> Si <sub>3</sub>	99.10±0.23	0.25±0.03	0.40±0.08	-----
L-Threonine	402-411	C <sub>18</sub> H <sub>42</sub> NO <sub>3</sub> Si <sub>3</sub>	99.82±0.04	0.34±0.01	0.26±0.02	-----
L-Alanine	258-267	C <sub>11</sub> H <sub>26</sub> NO <sub>2</sub> Si <sub>2</sub>	99.82±0.11	0.20±0.02	-----	-----
β-Alanine	258-267	C <sub>11</sub> H <sub>26</sub> NO <sub>2</sub> Si <sub>2</sub>	96.93±0.09	0.10±0.01	2.90±0.09	-----
<b>Small metabolites</b>						
Urea	229-238	C <sub>9</sub> H <sub>23</sub> N <sub>2</sub> O <sub>2</sub> Si <sub>2</sub>	99.49±0.10	0.16±0.01	0.03±0.01	0.24±0.09
Succinate	287-296	C <sub>12</sub> H <sub>25</sub> O <sub>4</sub> Si <sub>2</sub>	99.51±0.18	0.13±0.01	0.07±0.01	0.24±0.08
Fumarate	285-294	C <sub>12</sub> H <sub>23</sub> O <sub>4</sub> Si <sub>2</sub>	98.64±0.31	0.37±0.16	0.04±0.03	0.94±0.18
Malate	417-426	C <sub>18</sub> H <sub>39</sub> O <sub>5</sub> Si <sub>3</sub>	99.96±0.05	0.14±0.01	0.21±0.01	-----
Citrate	457-466	C <sub>20</sub> H <sub>39</sub> O <sub>6</sub> Si <sub>3</sub>	99.60±0.20	0.20±0.01	0.20±0.01	-----
Lactate	259-268	C <sub>11</sub> H <sub>25</sub> O <sub>3</sub> Si <sub>2</sub>	99.87±0.08	0.13±0.03	-----	-----
Ribulose 5P	381-390	C <sub>13</sub> H <sub>28</sub> O <sub>7</sub> Si <sub>2</sub> P	91.70±0.60	0.10±0.01	0.10±0.01	6.20±0.60
<b>Fatty acids</b>						
Lauric acid	255-264	C <sub>14</sub> H <sub>29</sub> O <sub>2</sub> Si	99.52±0.07	0.25±0.04	0.33±0.04	-----
Myristic acid	283-292	C <sub>16</sub> H <sub>33</sub> O <sub>2</sub> Si	99.55±0.05	0.04±0.01	0.46±0.03	-----
Palmitic acid	311-320	C <sub>18</sub> H <sub>37</sub> O <sub>2</sub> Si	98.36±0.19	0.05±0.01	0.50±0.03	0.86±0.17
Stearic acid	339-348	C <sub>20</sub> H <sub>41</sub> O <sub>2</sub> Si	97.59±0.19	0.04±0.01	0.65±0.02	1.56±0.20
Cholesterol	441-450	C <sub>29</sub> H <sub>51</sub> O <sub>2</sub> Si	95.89±0.19	0.33±0.05	0.46±0.04	2.34±0.21

759

760

761

762

763



764

765 **Table 3.** Theoretical abundance for the studied metabolites glycine, serine and L-alanine.

<b>Compound</b>	<b>Theoretical abundances</b>			
<i>Glycine (m/z)</i>	<b>Nat</b>	<sup>13</sup> <b>C<sub>1</sub></b>	<sup>13</sup> <b>C<sub>2</sub></b>	<sup>13</sup> <b>C<sub>3</sub></b>
244	0.0000	0.0000	0.0000	---
245	0.0000	0.0000	0.0000	---
246	0.7553	0.0041	0.0000	---
246	0.1638	0.7601	0.0084	---
247	0.0690	0.1568	0.7649	---
248	0.0099	0.0677	0.1497	---
249	0.0017	0.0092	0.0665	---
250	0.0001	0.0016	0.0085	---
251	0.0000	0.0001	0.0015	---
252	0.0000	0.0000	0.0001	---
<i>Serine (m/z)</i>	<b>nat</b>	<sup>13</sup> <b>C<sub>1</sub></b>	<sup>13</sup> <b>C<sub>2</sub></b>	<sup>13</sup> <b>C<sub>3</sub></b>
388	0.0000	0.0000	0.0000	0.0000
389	0.0000	0.0000	0.0000	0.0000
390	0.6433	0.0035	0.0000	0.0000
391	0.2223	0.6479	0.0071	0.0000
392	0.1038	0.2170	0.6524	0.0108
393	0.0238	0.1021	0.2117	0.6569
394	0.0055	0.0228	0.1005	0.2062
395	0.0008	0.0053	0.0219	0.0989
396	0.0001	0.0008	0.0051	0.0210
397	0.0000	0.0001	0.0007	0.0049
<i>L-Alanine (m/z)</i>	<b>nat</b>	<sup>13</sup> <b>C<sub>1</sub></b>	<sup>13</sup> <b>C<sub>2</sub></b>	<sup>13</sup> <b>C<sub>3</sub></b>
258	0.0000	0.0000	0.0000	0.0000
259	0.0000	0.0000	0.0000	0.0000
260	0.7470	0.0072	0.0000	0.0000
261	0.1702	0.7494	0.0145	0.0002
262	0.0700	0.1630	0.7517	0.0218
263	0.0105	0.0684	0.1557	0.7538
264	0.0018	0.0098	0.0669	0.1484
265	0.0001	0.0017	0.0091	0.0655
266	0.0000	0.0001	0.0016	0.0084
267	0.0000	0.0000	0.0001	0.0015

766

767

768

769

770

771

772

773

774 **Table 4.** Theoretical abundance for the studied metabolites glycine, serine and L-alanine calculated  
 775 taking into account the spectral purity of the selected clusters.

<b>Compound</b>	<b>Theoretical abundances</b>			
<i>Glycine (m/z)</i>	<b>Nat</b>	<sup>13</sup> <b>C<sub>1</sub></b>	<sup>13</sup> <b>C<sub>2</sub></b>	<sup>13</sup> <b>C<sub>3</sub></b>
244	0.0009	0.0000	0.0000	---
245	0.0038	0.0009	0.0000	---
246	0.7379	0.0080	0.0009	---
246	0.1730	0.7427	0.0121	---
247	0.0702	0.1663	0.7474	---
248	0.0108	0.0688	0.1594	---
249	0.0018	0.0101	0.0675	---
250	0.0001	0.0017	0.0095	---
251	0.0000	0.0001	0.0016	---
252	0.0000	0.0000	0.0001	---
<i>Serine (m/z)</i>	<b>nat</b>	<sup>13</sup> <b>C<sub>1</sub></b>	<sup>13</sup> <b>C<sub>2</sub></b>	<sup>13</sup> <b>C<sub>3</sub></b>
388	0.0025	0.0000	0.0000	0.0000
389	0.0024	0.0025	0.0000	0.0000
390	0.6385	0.0059	0.0026	0.0000
391	0.2206	0.6430	0.0095	0.0027
392	0.1030	0.2154	0.6475	0.0131
393	0.0236	0.1013	0.2101	0.6519
394	0.0055	0.0227	0.0997	0.2047
395	0.0008	0.0053	0.0217	0.0981
396	0.0001	0.0008	0.0051	0.0208
397	0.0000	0.0001	0.0007	0.0049
<i>L-Alanine (m/z)</i>	<b>nat</b>	<sup>13</sup> <b>C<sub>1</sub></b>	<sup>13</sup> <b>C<sub>2</sub></b>	<sup>13</sup> <b>C<sub>3</sub></b>
258	0	0	0	0
259	0.0014	0.0000	0.0000	0.0000
260	0.7460	0.0056	0.0000	0.0000
261	0.1701	0.7508	0.0098	0.0002
262	0.0699	0.1632	0.7555	0.0233
263	0.0105	0.0686	0.1563	0.7527
264	0.0018	0.0098	0.0673	0.1482
265	0.0001	0.0017	0.0091	0.0654
266	0.0000	0.0001	0.0016	0.0084
267	0.0000	0.0000	0.0001	0.0015

776

777

778 **Table 5.** Comparison of the theoretical molar fractions (%) with experimental molar fractions  
 779 calculated by the proposed methodology in different gravimetrically prepared mixtures of natural  
 780 Glucose and D-Glucose-2-<sup>13</sup>C<sub>1</sub>, D-Glucose-1,2-<sup>13</sup>C<sub>2</sub>, D-Glucose-1,2,3-<sup>13</sup>C<sub>3</sub> and D-Glucose-<sup>13</sup>C<sub>6</sub>.

781

Mixtures of natural Glucose and labelled Glucoses		X <sub>nat</sub> (%)	X <sup>13</sup> C <sub>1</sub> (%)	X <sup>13</sup> C <sub>2</sub> (%)	X <sup>13</sup> C <sub>3</sub> (%)	X <sup>13</sup> C <sub>5</sub> (%)
1	Theoretical	18.81±0.14	37.07±0.25	20.82±0.20	14.67±0.13	8.63±0.10
	Experimental	18.82±0.02	37.06±0.05	20.75±0.11	14.74±0.10	8.67±0.06
2	Theoretical	18.44±0.14	13.71±0.13	41.15±0.37	9.67±0.09	17.03±0.18
	Experimental	18.49±0.06	13.74±0.06	41.15±0.07	9.68±0.01	17.07±0.04
3	Theoretical	18.81±0.14	18.43±0.14	10.43±0.10	39.44±0.25	12.90±0.20
	Experimental	18.82±0.03	18.50±0.07	10.45±0.03	39.47±0.05	12.91±0.05
4	Theoretical	19.23±0.15	9.35±0.09	16.01±0.16	19.87±0.17	35.54±0.37
	Experimental	19.30±0.09	9.44±0.05	16.10±0.09	19.92±0.09	35.58±0.03
5	Theoretical	18.79±0.14	18.58±0.16	21.08±0.20	19.84±0.17	21.71±0.23
	Experimental	18.90±0.12	18.60±0.05	21.07±0.04	19.90±0.07	21.75±0.06
6	Theoretical	18.62±0.14	23.03±0.19	25.90±0.24	19.52±0.16	12.94±0.14
	Experimental	18.70±0.10	22.99±0.08	25.92±0.07	19.57±0.05	12.90±0.04
7	Theoretical	18.46±0.14	---	31.08±0.29	28.96±0.22	21.50±0.23
	Experimental	18.50±0.08	0.07±0.02	31.14±0.09	29.08±0.14	21.42±0.15
8	Theoretical	19.35±0.15	28.75±0.23	---	25.13±0.20	26.77±0.29
	Experimental	19.41±0.09	28.76±0.18	0.03±0.03	25.27±0.14	26.79±0.03
9	Theoretical	19.09±0.15	23.47±0.20	26.60±0.26	---	30.83±0.33
	Experimental	19.18±0.11	23.55±0.09	26.69±0.18	-0.04±0.02	30.87±0.05
10	Theoretical	18.06±0.14	13.53±0.13	35.36±0.33	33.05±0.24	---
	Experimental	18.06±0.04	13.43±0.11	35.34±0.04	33.07±0.12	0.08±0.01

782

783

784

785

786

787

788

789

790

791

792

793

794 **Table 6.** Comparison of the theoretical molar fractions with experimental molar fractions calculated  
 795 by the proposed methodology in different gravimetrically prepared mixtures of natural glycine and  
 796 labeled glycine.

Mixtures of natural glycine and glycine-2- <sup>13</sup> C <sub>1</sub>		X <sub>nat</sub> (%)	X <sup>13</sup> C <sub>1</sub> (%)	
1	Theoretical	99.03±0.01	0.97±0.01	
	Experimental	99.05±0.38	1.12±0.32	
2	Theoretical	90.34±0.11	9.66±0.11	
	Experimental	90.48±0.30	9.96±0.26	
3	Theoretical	80.41±0.21	19.59±0.21	
	Experimental	80.73±0.17	19.64±0.10	
4	Theoretical	75.63±0.24	24.37±0.24	
	Experimental	75.92±0.15	24.64±0.08	
5	Theoretical	50.69±0.33	49.31±0.33	
	Experimental	51.15±0.06	49.64±0.04	
Mixtures of natural glycine and glycine- <sup>13</sup> C <sub>2</sub>		X <sub>nat</sub> (%)	X <sup>13</sup> C <sub>2</sub> (%)	
1	Theoretical	99.11±0.01	0.89±0.01	
	Experimental	99.16±0.01	0.86±0.02	
2	Theoretical	91.02±0.10	8.98±0.10	
	Experimental	91.14±0.06	9.00±0.02	
3	Theoretical	80.14±0.18	19.86±0.18	
	Experimental	80.81±0.23	19.93±0.29	
4	Theoretical	76.32±0.21	23.68±0.21	
	Experimental	76.42±0.05	23.61±0.02	
5	Theoretical	52.39±0.29	47.61±0.29	
	Experimental	52.54±0.17	47.88±0.15	
Mixtures of natural glycine, glycine-2- <sup>13</sup> C <sub>1</sub> and glycine- <sup>13</sup> C <sub>2</sub>		X <sub>nat</sub> (%)	X <sup>13</sup> C <sub>1</sub> (%)	X <sup>13</sup> C <sub>2</sub> (%)
1	Theoretical	98.16±0.02	0.96±0.01	0.88±0.01
	Experimental	98.34±0.24	0.92±0.24	0.91±0.11
2	Theoretical	90.95±0.09	4.55±0.06	4.50±0.05
	Experimental	91.01±0.19	4.73±0.14	4.43±0.22
3	Theoretical	81.23±0.17	9.70±0.11	9.06±0.09
	Experimental	81.38±0.08	9.86±0.07	9.11±0.04
4	Theoretical	61.50±0.26	19.92±0.19	18.58±0.15
	Experimental	61.88±0.12	20.10±0.18	18.43±0.10
5	Theoretical	20.93±0.18	40.72±0.26	38.35±0.23
	Experimental	20.99±0.01	41.04±0.04	38.61±0.04

797

798

799

800

801

802

803 **Table 7.** Comparison of the theoretical molar fraction with experimental molar fraction calculated by  
 804 the proposed methodology in different gravimetrically prepared mixtures of natural Glycine and  
 805 Glycine-2-<sup>13</sup>C and natural Glycine Glycine-<sup>13</sup>C<sub>2</sub>.

806

<b>Mixtures of natural Glycine and Glycine-2-<sup>13</sup>C</b>		<b>X<sup>13</sup>C<sub>1</sub> (%)</b>
1	Theoretical	0.7094±0.0093
	Experimental	0.6852±0.0563
2	Theoretical	0.4750±0.0063
	Experimental	-1.2912±0.0047
3	Theoretical	0.2376±0.0031
	Experimental	-1.5389±0.0054
4	Theoretical	0.0962±0.0013
	Experimental	-1.7145±0.0109
<b>Mixtures of natural Glycine and Glycine-<sup>13</sup>C<sub>2</sub></b>		<b>X<sup>13</sup>C<sub>2</sub> (%)</b>
1	Theoretical	0.6694±0.0079
	Experimental	0.6752±0.0634
2	Theoretical	0.4592±0.0054
	Experimental	0.0823±0.0060
3	Theoretical	0.0900±0.0026
	Experimental	-0.1413±0.0287
4	Theoretical	0.0900±0.0011
	Experimental	-0.2737±0.0047

807

808

809

810

811

812

813

814

815

816 **Table 8.** Comparison of the  $^{13}\text{C}/^{12}\text{C}$  isotope ratios obtained by GC-C-IRMS with those obtained applying equation (1) and equation (3) for the intracellular  
 817 metabolites serine, malate, L-aspartate and L-glutamate in cultures of four different cell lines: PNT1A, PC3, LNCaP and LNCaP<sup>MOCK</sup>.

818

Compound	Cell Line	Molar Fractions				$^{13}\text{C}/^{12}\text{C}$ Ratio	$^{13}\text{C}/^{12}\text{C}$ Ratio
		X <sub>nat</sub> (%)	X <sup>13</sup> C <sub>1</sub> (%)	X <sup>13</sup> C <sub>2</sub> (%)	X <sup>13</sup> C <sub>3</sub> (%)	GC-MS	GC-C-IRMS
Serine	<i>PNT1A</i>	91.69±0.90	8.02±0.86	0.22±0.24	0.12±0.21	0.0150±0.0010	0.0153±0.0003
	<i>LNCaP</i>	78.43±0.54	20.61±0.43	1.16±0.09	----	0.0218±0.0010	0.0224±0.0009
	<i>PC3</i>	96.27±0.61	4.77±0.25	0.07±0.58	----	0.0130±0.0010	0.0132±0.0006
	<i>LNCaP<sup>MOCK</sup></i>	88.43±0.61	10.77±0.57	0.78±0.10	0.06±0.04	0.0214±0.0010	0.0217±0.0018
Malate	<i>PNT1A</i>	86.85±0.99	12.02±1.00	0.91±0.40	0.11±0.06	0.0176±0.0029	0.0176±0.0004
	<i>LNCaP</i>	70.73±0.84	25.79±0.85	2.68±0.25	----	0.0260±0.0013	0.0261±0.0003
	<i>PC3</i>	64.39±0.58	32.99±1.69	3.45±0.41	----	0.0290±0.0027	0.0296±0.0005
	<i>LNCaP<sup>MOCK</sup></i>	86.37±0.93	12.88±0.90	0.84±0.20	----	0.0231±0.0031	0.0248±0.0015
L-Aspartate	<i>PNT1A</i>	89.20±0.79	9.84±0.52	0.80±0.22	0.03±0.07	0.0160±0.0011	0.0158±0.0005
	<i>LNCaP</i>	72.96±0.91	24.40±0.95	2.02±0.23	0.05±0.06	0.0241±0.0013	0.0252±0.0012
	<i>PC3</i>	67.61±11.20	29.14±0.98	4.38±1.53	----	0.0271±0.0015	0.0289±0.0019
	<i>LNCaP<sup>MOCK</sup></i>	89.04±0.80	9.95±0.83	0.41±0.08	----	0.0220±0.0012	0.0228±0.0012
L-Glutamate	<i>PNT1A</i>	85.17±0.90	13.84±0.75	1.11±0.18	0.04±0.04	0.0177±0.0010	0.0184±0.0004
	<i>Lncap</i>	64.24±0.91	29.81±0.56	5.51±0.33	0.19±0.04	0.0293±0.0015	0.0310±0.0011
	<i>PC3</i>	55.38±0.63	35.82±0.77	8.53±0.17	0.34±0.16	0.0349±0.0012	0.0349±0.0011
	<i>LNCaP<sup>MOCK</sup></i>	87.36±1.21	11.27±1.06	1.10±0.20	----	0.0239±0.0013	0.0249±0.0008

819

820

821 **Table 9** Uncertainty budget of the measurement of the  $^{13}\text{C}/^{12}\text{C}$  isotope ratio of serine in PNT1A cell  
 822 line calculated from the molar fractions obtained by GC-MS and equation (3).

Uncertainty source	Contribution (%)
$^{13}\text{C}$ abundance in labeled serine	1.5
$^{12}\text{C}$ abundance in labeled serine	<0.1
Molar fraction for the natural abundance serine	<0.1
Molar fraction of a serine labeled in one $^{13}\text{C}$ atom ( $X^{13}\text{C}_1$ )	0.5
Molar fraction of a serine labeled in two $^{13}\text{C}$ atom ( $X^{13}\text{C}_2$ )	2.3
Molar fraction of a serine labeled in three $^{13}\text{C}$ atom ( $X^{13}\text{C}_3$ )	4.7
Natural abundance for $^{13}\text{C}$	91.0
Natural abundance for $^{12}\text{C}$	<0.1

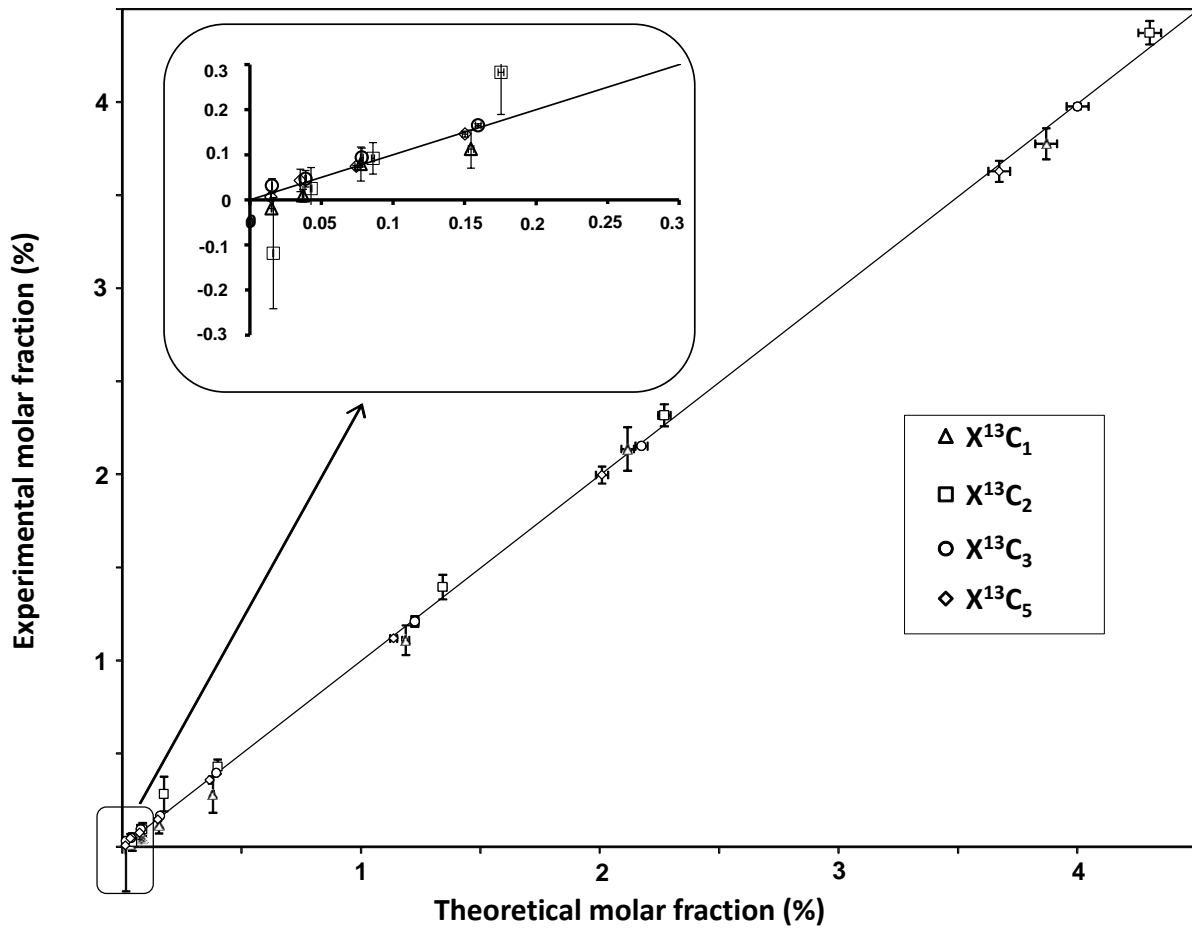
823

824 **Table 10.** Experimental abundances measured for the three studied metabolites in the PNT1A,  
 825 LNCaP, PC3, LNCaP<sup>MOCK</sup> and LNCaP<sup>S12</sup> cell lines. Values in brackets correspond to the relative  
 826 standard deviation (%) obtained from n=3 independent GC-MS injections.

Compound	Experimental abundances				
	PNT1A	LNCaP	PC3	LNCaP <sup>MOCK</sup>	LNCaP <sup>S12</sup>
<i>Glycine</i> (m/z)					
244	0.0114 (28.6)	0.0016 (16.2)	0.0110 (27.2)	0.0015 (11.1)	0.0011 (15.3)
245	0.0072 (35.3)	0.0034 (2.6)	0.0060 (11.9)	0.0032 (2.1)	0.0042 (17.6)
246	0.7040 (0.3)	0.6166 (0.7)	0.7054 (0.3)	0.6372 (0.2)	0.6504 (0.4)
246	0.1875 (2.4)	0.2664 (1.4)	0.1869 (0.7)	0.2505 (0.4)	0.2388 (1.1)
247	0.0712 (0.9)	0.0860 (0.7)	0.0720 (1.8)	0.0833 (0.1)	0.0824 (0.9)
248	0.0150 (1.5)	0.0213 (2.2)	0.0140 (26.4)	0.0198 (1.7)	0.0188 (3.8)
249	0.0025 (9.9)	0.0036 (9.7)	0.0033 (17.3)	0.0034 (4.5)	0.0032 (3.6)
250	0.0008 (53.7)	0.0007 (14.1)	0.0007 (32.4)	0.0006 (5.3)	0.0006 (14.2)
251	0.0000	0.0000	0.0001 (16.7)	0.0000	0.0001 (56.3)
252	0.0000	0.0000	0.0000	0.0000	0.0000
<i>Serine</i> (m/z)					
388	0.0042 (9.3)	0.0019 (3.0)	0.0000	0.0020 (4.7289%)	0.0017 (40.8)
389	0.0029 (6.2)	0.0035 (2.6)	0.0000	0.0035 (2.0469%)	0.0028 (35.5)
390	0.5865 (0.9)	0.4994 (0.7)	0.6118 (0.6)	0.5053 (0.5356%)	0.5231 (0.2)
391	0.2541 (1.4)	0.3067 (0.5)	0.2433 (0.8)	0.3034 (0.5648%)	0.2932 (0.7)
392	0.1135 (2.2)	0.1334 (0.7)	0.1111 (2.8)	0.1311 (0.1727%)	0.1280 (0.8)
393	0.0301 (2.6)	0.0420 (1.4)	0.0282 (11.6)	0.0417 (1.8579%)	0.0392 (0.9)
394	0.0070 (3.5)	0.0103 (2.4)	0.0054 (12.8)	0.0103 (2.1630%)	0.0093 (0.6)
395	0.0012 (8.3)	0.0020 (1.6)	0.0000	0.0020 (0.3145%)	0.0019 (1.7)
396	0.0000	0.0003 (4.5)	0.0000	0.0003 (12.6020%)	0.0003 (0.2)
397	0.0000	0.0000	0.0000	0.0000	0.0000
<i>L-Alanine</i> (m/z)					
258	0.0022 (3.1)	0.0019 (4.1)	0.0016 (16.2)	0.0015 (3.1)	0.0019 (9.9)
259	0.0068 (4.1)	0.0037 (5.3)	0.0060 (17.8)	0.0033 (8.4)	0.0048 (14.4)
260	0.5369 (1.0)	0.5030 (1.1)	0.5059 (5.3)	0.4657 (1.6)	0.5220 (0.7)
261	0.3265 (1.9)	0.3563 (0.8)	0.3928 (3.5)	0.3736 (1.6)	0.3297 (0.9)
262	0.0951 (1.3)	0.1056 (1.8)	0.0831 (55.7)	0.1134 (2.6)	0.1073 (3.3)
263	0.0274 (6.9)	0.0292 (4.8)	0.0103 (45.8)	0.0363 (7.2)	0.0288 (0.9)
264	0.0048 (2.7)	0.0000	0.0000	0.0059 (2.5)	0.0052 (0.6)
265	0.0000	0.0000	0.0000	0.0000	0.0000
266	0.0000	0.0000	0.0000	0.0000	0.0000
267	0.0000	0.0000	0.0000	0.0000	0.0000

827 **FIGURES**

828 **Figure 1.** Comparison between the theoretical molar fractions (%) with the experimental molar  
829 fraction determined by the proposed methodology in different gravimetrically prepared mixtures of  
830 natural glucose and D-glucose-2-<sup>13</sup>C<sub>1</sub>, D-glucose-1,2-<sup>13</sup>C<sub>2</sub>, D-glucose-1,2,3-<sup>13</sup>C<sub>3</sub> and D-glucose-<sup>13</sup>C<sub>6</sub>.  
831 The line corresponds to a slope of 1 (perfect agreement).

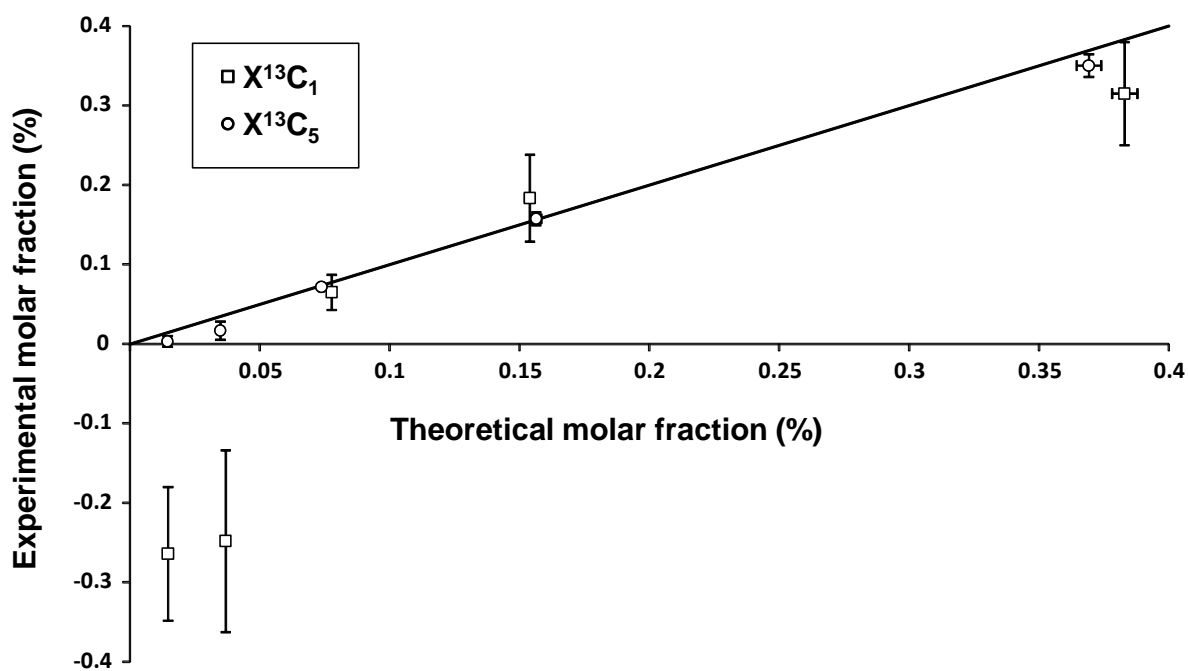


832  
833  
834  
835  
836  
837  
838  
839  
840



841 **Figure 2.** Comparison of the theoretical molar fraction with experimental molar fraction calculated by  
842 the proposed methodology in different gravimetrically prepared mixtures of a) natural glucose and D-  
843 glucose-2- $^{13}\text{C}_1$  and b) natural glucose and D-glucose- $^{13}\text{C}_6$ . The line corresponds to a slope of 1  
844 (perfect agreement)

845



846

847

848

849

850

851

852

853

854

855

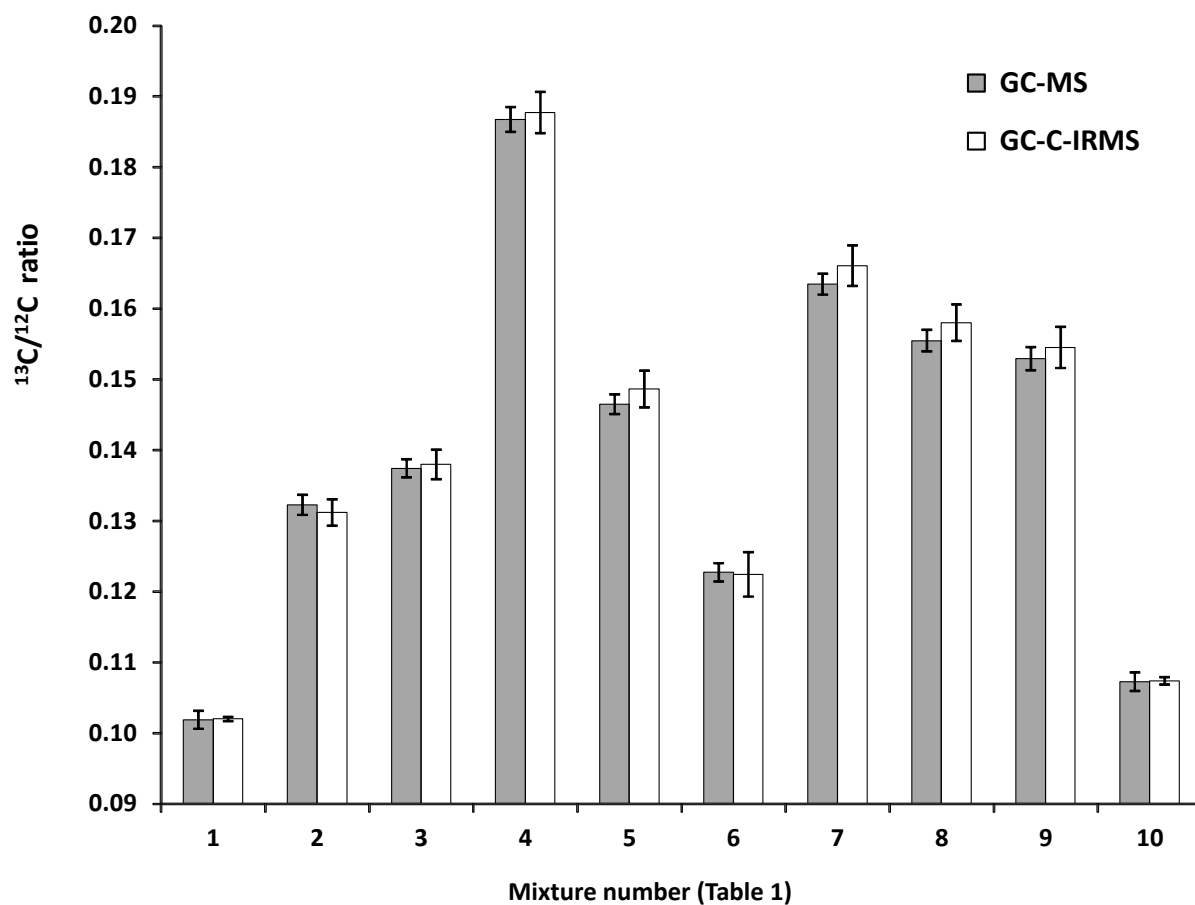
856

857

858

859 **Figure 3.** Comparison of the  $^{13}\text{C}/^{12}\text{C}$  isotope ratios obtained by GC-C-IRMS with those obtained by  
860 GC-MS applying equation (1) and equation (3) for the ten mixtures of Table 5 containing natural  
861 abundance D-glucose, D-glucose-2- $^{13}\text{C}_1$ , D-glucose-1,2- $^{13}\text{C}_2$ , D-glucose-1,2,3- $^{13}\text{C}_3$  and D-glucose-  
862  $^{13}\text{C}_6$ .

863



864

865

866

867

868

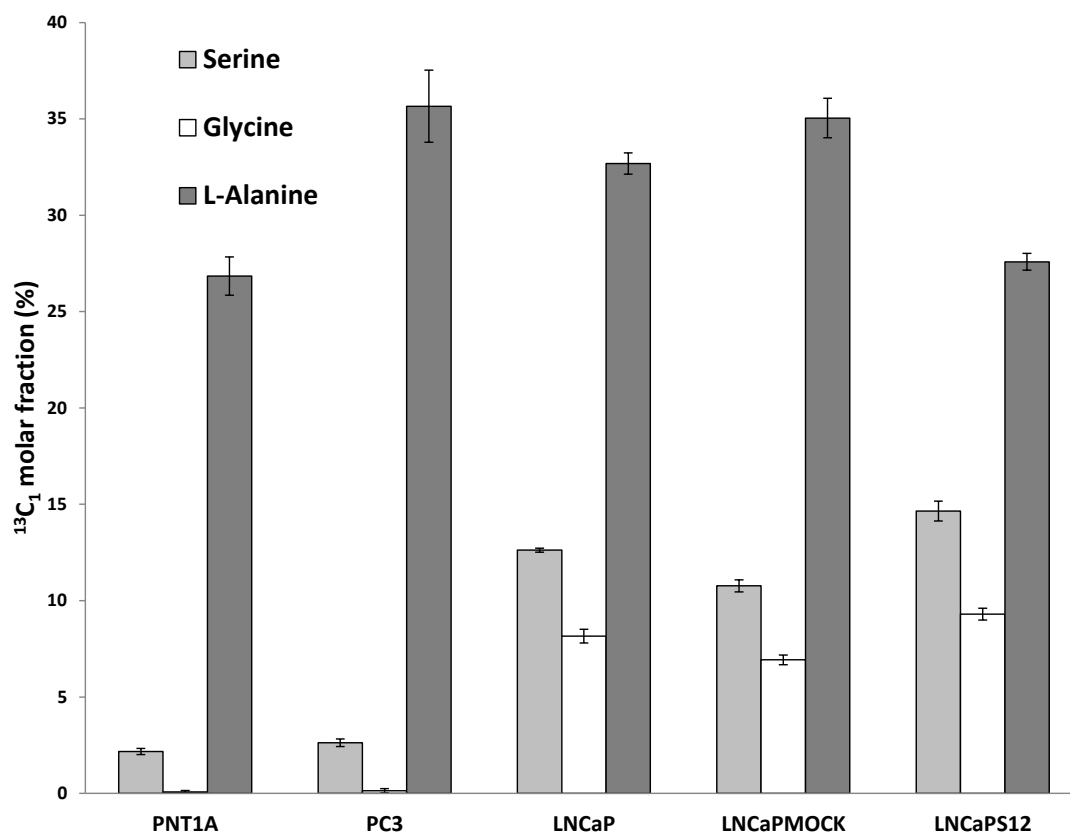
869

870

871

872 **Figure 4:** Molar fraction for the  $^{13}\text{C}_1$ -analogue of serine, glycine and L-alanine measured in cell  
873 cultures of normal human prostate epithelium PNT1A cells and four different prostate cancer cell  
874 lines: PC3, LNCaP, LNCaP<sup>S12</sup>, and LNCaP<sup>MOCK</sup>.

875



876

877

878

879

880